

RIGA TECHNICAL UNIVERSITY
Faculty of Mechanical Engineering, Transport and Aeronautics
Institute of Aeronautics

Kristīne CARJOVA

PhD Student of the Doctoral Study Programme “Transport”

**HELICOPTER STRUCTURE FATIGUE DEFECT
ACOUSTIC DIAGNOSTICS WITH DEFECT LOCALIZATION**

Summary of the Doctoral Thesis

Scientific supervisor
Dr. habil. sc. ing., Professor
A. URBAHS

**RTU Press
Riga 2016**

Carjova K. Helicopter Structure Fatigue Defect
Acoustic Diagnostics with Defect Localization.
Summary of the Doctoral Thesis. – Rīga: RTU Press,
2016. – 61 p.

Printed according to the Resolution No. P-22 of the
RTU Science Board as of 10 March 2016, Minutes
No.1/2016/



The present research has been supported by the European Social Fund within the project
“Support for the Implementation of Doctoral Studies at Riga Technical University”.

ISBN 978-9934-10-805-1

**DOCTORAL THESIS PROPOSED TO RIGA TECHNICAL
UNIVERSITY FOR THE PROMOTION TO THE SCIENTIFIC DEGREE
OF DOCTOR OF ENGINEERING SCIENCES**

To be granted the scientific degree of Doctor of Engineering Sciences, the present Doctoral Thesis has been submitted for the defence at the open meeting of RTU Promotion Council on 9th of June 2016, Room 218, at the Institute of Aeronautics, Riga Technical University, Lomonosova street 1A, k-1, Riga.

OFFICIAL REVIEWERS

Professor, *Dr. habil. sc. ing.* Vladimirs ŠESTAKOVŠ
Riga Technical University, Latvia

Professor, *Dr. habil. sc. ing.* Juris CIMANSKIS
Latvian Maritime Academy, Latvia

Professor, *Dr. habil. sc. ing.* Jonas STANKŪNAS
Vilnius Gediminas Technical University,
Director of Antanas Gustaitis' Aviation Institute, Lithuania

DECLARATION OF ACADEMIC INTEGRITY

I hereby declare that the Doctoral Thesis submitted for the review to Riga Technical University for the promotion to the scientific degree of Doctor of Engineering Sciences is my own and does not contain any unacknowledged material from any source. I confirm that this Thesis has not been submitted to any other university for the promotion to other scientific degree.

Kristīne Carjova (Signature)

Date:

The Doctoral Thesis has been written in Latvian. It consists of an introduction, 5 chapters, conclusions, bibliography with 213 reference sources, 3 annexes, 193 figures, 6 tables, and 38 formulae. The volume of the present Thesis is 205 pages.

CONTENTS

GENERAL DESCRIPTION OF THE DOCTORAL THESIS	6
Topicality of the Doctoral Thesis.....	6
The Aim and objectives of the Doctoral Thesis.....	6
Research methods.....	7
Research objects.....	7
Scientific novelty and principal research results.....	7
Practical application of the Doctoral Thesis	8
Topics to be defended in the Doctoral Thesis.....	8
The author in this Thesis defends:	8
Thesis approbation	8
The structure and content of the Doctoral Thesis	12
The content of the Doctoral Thesis	12
1. ANALYSIS OF AIRCRAFT FUSELAGE FATIGUE DEFECTS AND METHODS USED FOR THEIR DETECTION	13
1.1 Helicopter load analysis during operation.....	13
1.2 Helicopter structural element defect in operation analysis.....	13
1.3 Acoustic emission control method for structural fatigue damage.....	15
2. EXPERIMENTAL RESEARCH METHODOLOGY AND PROVISION OF ACOUSTIC EMISSION MEASUREMENT EQUIPMENT	16
2.1 Acoustic emission signal recording and processing.....	16
2.2 Characteristics of the research object.....	17
2.3 Experimental sample bench testing and procedure methodology	18
2.4 Helicopter structure bench testing methodology and equipment	20
3. MATHEMATICAL MODEL OF FATIGUE DEFECT LOCALIZATION FOR MATERIALS AND STRUCTURES	23
3.1 Defect localization on the plane based on time difference of signal arrival.....	23

3.2 Mathematical model for fatigue defect localization in aviation structures based on AE signal amplitude	24
4. EXPERIMENTAL RESEARCH ON AVIATION STRUCTURAL MATERIAL SAMPLES USING ACOUSTIC EMISSION METHOD.....	27
4.1 Experimental research on samples made from aluminium alloy under static and dynamic loading	27
4.2 Experimental research on composite material damageability under cyclic loading	29
5. HELICOPTER STRUCTURE FATIGUE DAMAGE DIAGNOSTICS WITH DEFECT LOCALIZATION	31
5.1 Analysis of AE signal propagation features in helicopter structural elements.....	31
5.2 Diagnostics of bolted joints using the acoustic emission method during helicopter bench tests	37
5.3 Evaluation of the defects of riveted connections.....	45
CONCLUSIONS.....	50
REFERENCES.....	52

GENERAL DESCRIPTION OF THE DOCTORAL THESIS

Topicality of the Doctoral Thesis

Aviation structure failures mostly relate to fatigue damage accumulation and fatigue crack development. Therefore, one of the most important issues in assessing fatigue is development of scientifically based methods for fatigue damage evaluation and structural elements' lifetime calculation in variable load conditions. These methods make it possible to choose the optimum shape and size of the structure at the design stage and to control the real process of damage accumulation in structures during their operation.

In point of structure load-bearing capacity, when a large part of its resource structural material is operated with defects but the operation time is determined by defect development time until its critical dimensions, the methods that make it possible to detect the defects at an early stage and to predict the remaining structures with cracks resources become actual.

One of the perspective diagnostic methods that allow dealing with these tasks is the acoustic non-destructive testing method based on the acoustic emission (AE) signal parameter analysis. The practical use of this method is related to the interpretation of the diagnostic measurement data.

Protruding problem must be solved by theoretical and practical research of defect origination and development obtained from AE information reading, interpretation and localization, which is recorded in the diagnostic object.

The Aim and objectives of the Doctoral Thesis

During analysis of fatigue defects in aircraft structures and diagnostic methods used for their detection, the following aim of the Thesis is set: *to develop acoustic diagnostic methodology with defect localization for a helicopter structure*. To achieve this aim, the following objectives are defined:

- 1) to perform a helicopter operating defect analysis and evaluate the non-destructive testing and diagnostic methods used for defect detection;
- 2) to develop a multi-channel acoustic emission measurement and data processing methodology for the material and structure defectology analysis at static and dynamic load conditions;
- 3) to develop a mathematical model of material and structural fatigue defect localization based on the AE measurement data and taking into account the real impact of structural elements;

- 4) to evaluate the AE parameters informativity for the metallic and composite material structures defectology control at static and dynamic load conditions based on the experimental studies;
- 5) to determine AE parameters for defect localization in the helicopter structure taking into account the real impact of structural elements based on the experimental studies;
- 6) to perform fatigue defect diagnostics in the helicopter fuselage and tail boom jointing frames with defect localization in bolts based on the AE measurement data;
- 7) to develop a rivet and bolt joint AE testing methodology in real structures based on AE measurements;
- 8) to make fractographic analysis of the fatigue fracture of structure elements and to identify AE parameter correlation by means of fracture kinetics during helicopter bench tests.

Research methods

Research methodology and research methods:

theoretical methods:

- mathematical modeling,
- rigid body physics,
- mathematical statistics and correlation analysis,
- probability and reliability theory;

experimental methods:

- AE signal measurement with AE equipment according to the standards LVS EN 13554:2011 and LVS EN 1330-9:2009,
- AE data processing using specialized software,
- material fatigue fracture fractographic analysis,
- material microstructure experimental research,
- experimental research of material chemical composition,
- statistical processing of experimental research results.

Research objects

- Aluminum alloy and composite samples
- Helicopter structures
- Full-scale helicopter fatigue bench

Scientific novelty and principal research results

The following innovative solutions were developed during the research:

- mathematical model of structural fatigue defect localization taking into account the real impact of structural elements;
- methodology of structural rivet and bolt joints control using AE method;
- results of AE diagnostics of helicopter fuselage and tail boom jointing bolts based on an experimental research;
- defect fractographic analysis and their feature identification with the AE measurement methodology.

Practical application of the Doctoral Thesis

Results of the Doctoral Thesis has a broad practical relevance and application, as within its framework the new and highly efficient defect localization by AE signal amplitude method was developed. This method makes it possible to determine the location of the defect cluster center coordinates. In addition, this method can be deployed in defect localization for real structure bench tests. The obtained results are the basis of the development of diagnostic methodology for the helicopter structures in operation.

The results of the Thesis can be used in scientific fields such as technical diagnostics, non-destructive testing, rigid body mechanics, fracture mechanics, etc.

Topics to be defended in the Doctoral Thesis

The author in this Thesis defends:

- 1) experimental methodology for assessing structure damage with defect localization;
- 2) results of the diagnostics of the helicopter fuselage and tail boom joint bolts;
- 3) mathematical model of structural fatigue defect localization;
- 4) results of the metallic and composite sample experimental studies;
- 5) results of fractographic research.

Thesis approbation

Research results have been reported in 7 international scientific conferences:

- 1) Mechanika 2015: 20th International Scientific Conference, Lithuania, Kaunas, 23–24 April;
- 2) 17th International Conference of Transport Means, 23–24 October, 2014, Kaunas, Lithuania;
- 3) 11th International Seminar “Research and Education in Aircraft Design 2014”, 15–17 October, 2014, Vilnius, Lithuania;
- 4) 16th International Conference Transport Means, 25–26 October, 2013, Kaunas, Lithuania;

- 5) International Congress on Engineering and Technology, 25–27 June, 2013 Dubrovnik, Croatia;
- 6) Riga Technical University, 53rd International Scientific Conference, 11–12 October 2012, Riga;
- 7) Composite Mechanics, Riga, 28 May – 1 June 2012.

The research results have been published in 9 scientific papers:

- 1) Urbahs, A., Banov, M., Carjova, K., Rēdmāne, A., Feshchuk, Y., Banov, L. Features of the Acoustic Emission Control for the Monitoring of Pipeline System of Oil Heater Boilers. In: *Mechanika 2012: Proceedings of the 17th International Conference*, Lithuania, Kaunas, 12–13 April 2012. Kaunas: Technologija, 2012, pp. 334–337. ISSN 1822-2951;
- 2) Urbahs, A., Shanyavskiy, A., Banovs, M., Carjova, K. Evaluation of an Acoustic Emission Criterion of Under Surface Fatigue Cracks Development Mechanism in Metals. In: *Transport Means 2012: Proceedings of the 16th International Conference*, Lithuania, Kaunas, 25–26 October 2012. Kaunas: Technologija, 2012, pp. 131–134. ISSN 1822-296X;
- 3) Urbahs, A., Banovs, M., Carjova, K., Turko, V. The Characteristic Features of Composite Materials Specimen's Static Fracture Investigated by the Acoustic Emission Method. *Applied Mechanics and Materials*, 2012, Vol. 232, pp. 28–32. ISSN 1660-9336. Accessible at: doi:10.4028/www.scientific.net/AMM.232.28;
- 4) Urbahs, A., Banovs, M., Nasibullins, A., Carjova, K. Analysis of the Mechanism of Destruction of Aircraft Components. *Journal of Engineering and Technology*, Vol. 1, 2013, pp. 167–172. ISSN 1338-2330;
- 5) Shaniavski, A., Urbahs, A., Banovs, M., Nasibullins, A., Carjova, K. Analysis of the Mechanism of Destruction of Aircraft Components. In *Proceedings: International Congress on Engineering and Technology, Croatia, Dubrovnik, 25–27 June 2013*, pp. 167–172. ISBN 9788087670088;
- 6) Carjova, K., Urbaha, J. The Experimental Research of Titanium Alloys with Fragile Inclusions Mechanism Destruction. In: *Transport Means 2013: Proceedings of the 17th International Conference*, Lithuania, Kaunas, 24–25 October 2013. Kaunas: Technologija, 2013, pp. 197–200. ISSN 1822-296X;

- 7) Urbahs, A., Savkovs, K., Urbaha, M., Carjova, K. Heat and Erosion-Resistant Nanostructured Coatings for Gas Turbine Engines. In: *Aviation*, Vol. 17, Iss. 4, 2013, pp. 137–144. ISSN 1648-7788; e-ISSN 1822-4180. Accessible at: doi:10.3846/16487788.2013.861225;
- 8) Urbahs, A., Valberga, A., Banovs, M., Carjova, K., Stelpa, I. The Analysis of Efficiency of Acoustic Emission Diagnostic Method for the Determination of Defect Coordinates. In: *Transport and Aerospace Engineering*, No. 1, 2014, pp. 32–36. ISSN 2255-968X. Accessible at: doi:10.7250/tae.2014.006;
- 9) Urbahs, A., Carjova, K., Feščuks, J., Stelpa, I. Development of Theoretical Model for Aircraft Structural Health Monitoring by Acoustic Emission Method. In: *Mechanika 2015: Proceedings of the 20th International Conference*, Lithuania, Kaunas, 23–24 April 2015. Kaunas: Kaunas University of Technology, 2015, pp. 262–267. ISSN 1822-2951.

The research results have been submitted in 9 scientific papers:

- 1) Urbahs A., Banov M., Carjova K., Fescuks J. Structural health monitoring of helicopter bolted and riveted joints by acoustic emission method. **Submitted in:** *Aerospace Science and Technology*, 2016;
- 2) Urbahs A., Banovs M., Carjova K., Turko V., Feshchuk J. Research of the micromechanics of composite materials with polymer matrix failure under static loading by the acoustic emission method. **Submitted in:** *Aviation*, 2016;
- 3) Urbahs A., Carjova K. Research on bolting elements of helicopter fuselage and tail boom joints using acoustic emission amplitude and absolute energy criterion. **Submitted in:** *Advances in Acoustics and Vibration*, 2016;
- 4) Urbahs A., Carjova K., Feščuks J., Lama M. Research on Aluminium alloys static testing using Acoustic Emission testing. **Submitted in:** *Mechanika*, 2016;
- 5) Urbahs A., Carjova K., Feščuks J., Stelpa I. Analysing the results of acoustic emission diagnostics of a structure during helicopter fatigue tests. **Submitted in:** *Aviation*, 2016;
- 6) Urbahs A., Carjova K., Nasibullins A., Feščuks J. Research on fatigue fracture kinetics of helicopter fuselage bolting elements. **Submitted in:** *Transport Means 2016: Proceedings of the 20th International Conference*;

- 7) Urbahs A., Carjova K., Nasibullins A., Nedelko D., Millere E. Research on AE signal propagation in helicopter structural elements. **Submitted in:** *Transport and Aerospace engineering*, 2016;
- 8) Urbahs A., Carjova K., Urbaha M. Acoustic emission criterion during dynamic test of Aluminium alloys. **Submitted in:** *2016 AES-ATEMA International Conference "Advances and Trends in Engineering Materials and their Applications"*;
- 9) Urbahs A., Carjova K., Urbaha M. Acoustic emission diagnostics of fuselage and tail boom jointing bolts during helicopter bench tests. **Submitted in:** *ICAETM 2016: 18th International Conference on Aviation Engineering, Technology and Management*.

Received patents:

- 1) RIGAS TEHNISKA UNIVERSITATE. *A method for renovation of steel precision pair parts*. Urbahs A., Savkovs K., Urbaha M., Nesterovskis V., Carjova K., Urbaha J., Kuļešovs N. (inventors). Int. Cl.: C23C14/02, B23P6/00, C23C14/06, C23C14/34, C23C14/58. Application date: 2013-09-19. Patents and trade marks. EP2851450. 2015-03-25;
- 2) RIGAS TEHNISKA UNIVERSITATE. *Method for ultrasonic testing of bolted and riveted joints in structures*. Urbahs A., Banovs M., Urbaha M., Carjova K., Feščuks J. (inventors). Int. Cl.: G01N29/14. Application date 2013-10-31. Patents and trade marks. LV14971B. 2015-08-20;
- 3) RIGAS TEHNISKA UNIVERSITATE. *Method of defect localization using acoustic emission*. Urbahs A., Carjova K., Feščuks J., Urbaha M. (inventors). Int. Cl.P-16-35. Application date: 26-04-2016. Patents and trade marks. P-16-35.

The results of the Doctoral Thesis have been used in 6 scientific projects:

- 1) European Space Agency project "Development of the prototype of autonomous aerospace vehicle for comprehensive monitoring (DREAM) – Feasibility Study" – researcher (2015–2016);
- 2) Wear resistant nanostructured coatings for titanium joints, No. LZP 12.110 – researcher (2014–2016);
- 3) ERDAF project "Development of an experimental long flight distance unmanned aerial vehicle prototype for multi-purpose environmental monitoring (LARIDAE)", 2014/0029/2DP/2.1.1.1/14/APIA/VIAA/088 – researcher (2014–2015);

- 4) FP 7 “Transport (including Aeronautics)” programme (Call FP7-AAT-2012-RTD-L0) project “A novel concept of an extremely short take-off and landing all-surface (ESTOLAS) hybrid aircraft: from a light passenger aircraft to a very high payload cargo/pasenger version” – research assistant (2012–2014);
- 5) LZP 10.009 “Development of nanostructured multicomponent coating deposition technology” – research assistant (2012–2014);
- 6) ERDF project “Development of an unmanned aircraft system and creation of the industrial prototypes of unmanned aerial vehicles for performing the tasks of Latvian national economy” – research asisstant (2011–2013).

The structure and content of the Doctoral Thesis

The Doctoral Thesis is written in Latvian. It consists of an introduction, 5 chapters, conclusions, bibliography with 213 sources, 3 annexes, 193 figures, 6 tables, and 38 formulae. The total volume of the Thesis is 205 pages.

The content of the Doctoral Thesis

Introduction

Taking into account the aircraft loads during flight time, especially helicopter load during maneuvers, it is important to evaluate both the static and dynamic structural strength of the structure. Selected damage evaluation method must be such that in addition to the loads acting on the helicopters, other factors that may affect the structural strength and lifetime would be taken into account. The applied calculation method of loads differs from the calculation method for the flight tests, because there are different types of helicopters and the effect of loads on their structure is also different. Besides, even the load values obtained in real experiments cannot be assigned to particular helicopter flights.

Evaluating the non-destructive testing and diagnostic methods it is concluded that AE methods have advantages over other methods used for helicopter structure control. The nature of the AE method is analyzed in relationship with the informative capacity of registered parameters. The following main defect analysis AE parameters – AE signal amplitude, sum counts, absolute energy and intensity – are set forward as defect-characterizing criterions.

Despite the fact that there exist theoretical models that link AE parameters with defect occurrence and its stage of development, due to complex data processing they are still incomplete or their application for different materials and real structures in operation is not possible.

1. ANALYSIS OF AIRCRAFT FUSELAGE FATIGUE DEFECTS AND METHODS USED FOR THEIR DETECTION

1.1 Helicopter load analysis during operation

In order to ensure flight safety, an aircraft structure must be sufficiently safe and resistant to the pressures exerted on it during operation. It is necessary that strength and toughness is ensured throughout the entire aircraft exploitation at the potentially lowest construction weight [10, 12, 87–89].

Under these circumstances, the following conditions may be added to the baseloads acting on the parts of the aircraft [15, 24, 27, 34-36, 45, 53, 64, 65, 85, 86, 89]:

- raised pressure loads in sealed compartments;
- loads associated with the structure part fluctuations and large deformations (fluctuations caused by engine unbalance; acoustic oscillations; bearing surface deformation and fluctuation increment at interaction of aerodynamic and elastic forces, etc.);
- strength exposure that arises from the heated structure (in engine mounting area during supersonic flight).

When assessing the structural condition, the following factors affecting structural strength, reliability, and durability should be taken into consideration along with loads: wear and tear of parts, environmental effects (various forms of corrosion), change in material properties because of the heat, radiation, and other factors.

Different aircrafts have different load specifics. Helicopter load peculiarities are analyzed when helicopter is in flight. During the flight, the helicopter's flight curve is exposed to the surface and mass forces [15, 24, 27, 34–36, 45, 53, 64, 65, 85, 86, 89].

1.2 Helicopter structural element defect in operation analysis

Structural changes in the aircraft are caused by such factors as multiple load recurrence and thermal and environmental physico-chemical properties. Each of these factors creates a certain unfavorable effect on aircraft structures. Multiple load exposure creates [1–4, 5, 7, 8, 10, 28, 89, 90]:

- fatigue cracks and development, movable joint wear;
- free movement occurrence, slackening of riveted joints, and negative allowance connection.

The most common defects of aircraft fuselage structural parts are fatigue cracks and corrosion damage [73].

Helicopter structural elements defects in operation are known and analyzed already during the design stage, thus giving an insight into the expected defects and their timely elimination and repair.

Apart from the MI group, helicopter manufacturer's warnings about the MI-2, MI-24, MI-6 and MI-8 [3, 76–81, 84, 94] type helicopter tail boom jointing elements are very much prone to fatigue cracks.

These examples show the need to establish a fatigue damage likelihood of helicopter operation in between the repair periods. Also fatigue crack growth duration and kinetics are determined on the data of the existing model helicopters [94].

The fatigue cracking forecasting approach is very relative and can be applied only to a particular helicopter type, specific load conditions, and a particular structure. Fatigue cracks control in operation in real-time regime provides a more efficient crack appearance and growth control, thus providing helicopter repair at the existing conditions rather than at certain in-between repair periods when fatigue cracks growth in size is critical and may not be determined during the repair using traditional methods.

The analysis of existing diagnosis and non-destructive testing methods used for aircraft structure diagnostics. Recent scientific diagnostic and non-destructive testing methods make it possible to evaluate and analyze the research object without causing damage to it.

The diagnostic and non-destructive testing methods are widely used in science and industry including the field of aviation [1, 2–4, 6, 7, 13, 18, 22, 30]. The diagnostic and non-destructive control method is of vital importance in the aviation field. The Doctoral Thesis is devoted to the following non-destructive control methods: visual and optical, capillar, magnetic, eddy current, radiography, and acoustic methods. The most widely used diagnostic method is the vibration diagnostic method [39]. Nowadays, acoustic diagnostic techniques are particularly developing in non-destructive testing of aviation structures [1–4, 6–7, 17, 30–32, 39–66].

Acoustic emission method in the diagnostics of aviation industry at experimental level is used in different aviation structure diagnostics. AE has been used in the control of engine combustion chamber and casing [37], aircraft landing gear [4, 40, 41] and fuselage elements [1, 6, 7, 41, 69, 72, 96] for decades. Also, the acoustic emission method is one of the most advanced methods for space equipment non-destructive testing – in rocket nacelle and casing control [26, 37, 69, 72, 74], in multipurpose space craft thermal protection control [21], in assessment of lightning impact [6, 93], etc.

From 1970s until present, special on-board AE control systems are being developed to detect fatigue cracks and to control their development in the fuselage and other aircraft structural

elements during the flight [25, 29]. These systems have high sensitivity and they allow reliable determining of fatigue cracks in hardly accessible places; however, they are still not integrated [6, 93]. Taking into account its high potential, the acoustic emission method can be linked to the future diagnostics method for aircrafts in operation. There is significant elaboration in structural health monitoring (SHM) systems; however, because of the complex data reading they are still being comprehensively developed in civil aircraft fleet only at approbation level [36, 50, 58].

The AE method provides only dangerous, i.e., existing in the development process, defect identification and registration. AE method has a high sensitivity to the development process of existing defects. Its sensitivity is by far the most sensitive compared to other methods [6, 9, 11, 14]. The AE method is integral, i.e., one or more AE sensors that are rigidly mounted on the surface of an object can control the whole object without application of scanning. In such a way, complicated aircraft structures can be controlled by providing presence of several sensors and controlling the whole aircraft structure at the same time [7, 58, 63, 66].

The AE method, compared to other methods, has fewer restrictions for the material structure and properties. The method has been successfully used in the diagnostics of the material state, for which the use of other methods is impossible or difficult. It is possible to develop a control methodology for the AE method. The results can be quickly and easily read, the method is not time-consuming, and an object can be controlled without human presence.

For further research realization, the acoustic emission-destructive control method is selected as the most appropriate for aircraft structure fatigue defect diagnostics with its localization and methodology development. This is substantiated by the acoustic methods physical nature, diagnostic peculiarities and advantages in section 1.5 of the present Thesis.

1.3 Acoustic emission control method for structural fatigue damage

AE signals are characterized by some parameters, each of which is related to the physical process accompanied by AE, and their measurements can provide information on the research object or control condition. Let us analyze the informativity degree of the main parameters of the AE signal.

AE signals are characterized by amplitude, duration, form, and rise time (Fig. 1.1.). Similarly, the signal flow can be characterized by the event's statistical average frequency, spectral density, amplitude and time dispersion, average value, and dispersion. Each of the mentioned characteristics is related to the physical process caused by AE, and its determination can provide information on the condition of the object.

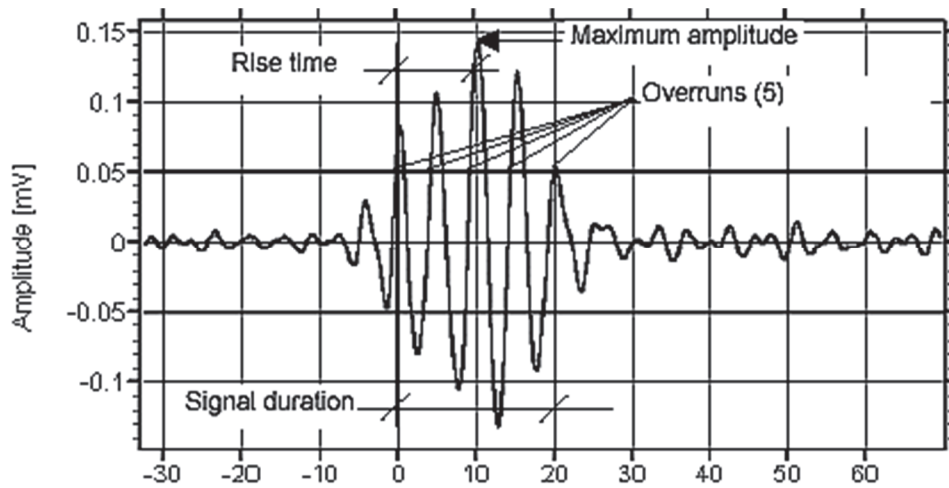


Fig. 1.1. AE parameters.

Also, AE signals are characterized by the total number of impulses and the AE activity [6, 82, 83, 92, 93]. These parameters allow obtaining additional information on the deformation and fracture process kinetics in the research object, which is exposed to external forces.

Despite the fact that research studies on the quantitative and qualitative link determination between the AE parameters and defect concentration nature in material samples and structure elements were launched decades ago [82, 93], there are still many unresolved issues due to complex data processing and interpretation [45, 48]. This is related to the use of AE perspective for early crack detection, the evaluation of crack growth kinetics, and the size of actual measurements in their test time or operation when traditional control methods cannot be applied [6, 93].

2. EXPERIMENTAL RESEARCH METHODOLOGY AND PROVISION OF ACOUSTIC EMISSION MEASUREMENT EQUIPMENT

2.1 Acoustic emission signal recording and processing

During research, the following devices were used: the multi-channel AE control equipment *PAC Pocket AE-2* [71], and *A-Line 32D (DDM)* [97]. The AE control device *PAC Pocket AE-2*, manufactured by *Physical Acoustics Corporation*, has “hit-based” architecture and is a portable, hand-held, 2-channel AE facility. *A-Line 32D (DDM)* is a digital multi-channel acoustic emission measurement system for acoustic emission data recording and processing.

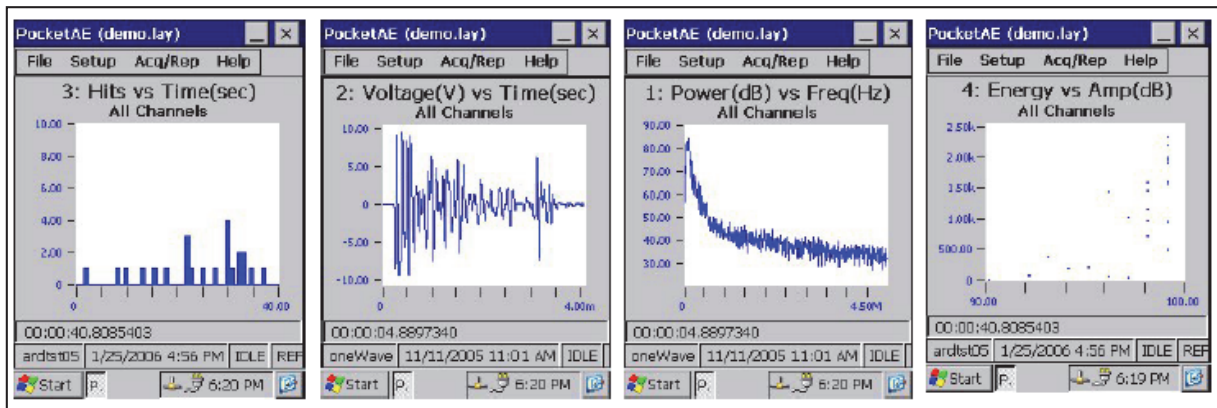


Fig. 2.1. Possibilities of the *PAC Pocket AE-2* graph.

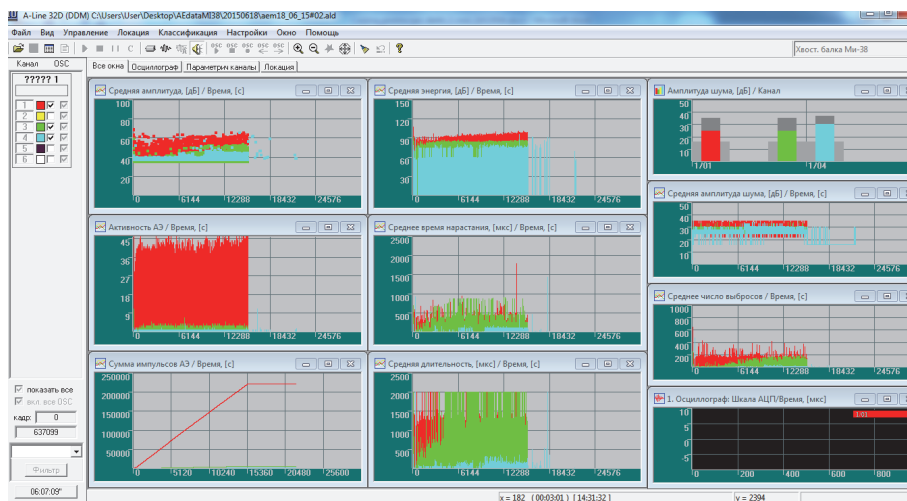


Fig. 2.2. *A-Line 32D (DDM)* visualization.

2.2 Characteristics of the research object

Aluminium samples

During the research [56, 61], aluminium samples (V95 alloy) were used.

Composite material samples

Two sample (made from glass fiber) groups were subject to tensile studies. The first group consists of samples in which the base of the fibers is oriented in the transverse direction relative to the force. The second group consists of the same samples but in which the fibers are oriented in the longitudinal direction relative to the force. In addition, for the second glass fiber sample group, the samples from carbon fiber were included. The samples are rectangular plates with lining attached to the upper and lower end under traverse testing machine clamps/presses. Tensometry transceiver and AE sensor were previously glued on the samples [49, 50].

Characteristics of the helicopter fuselage and tail boom

In general, the fuselage (Fig. 2.3.) strength scheme includes a coating consisting of longitudinal and traverse bonding elements.

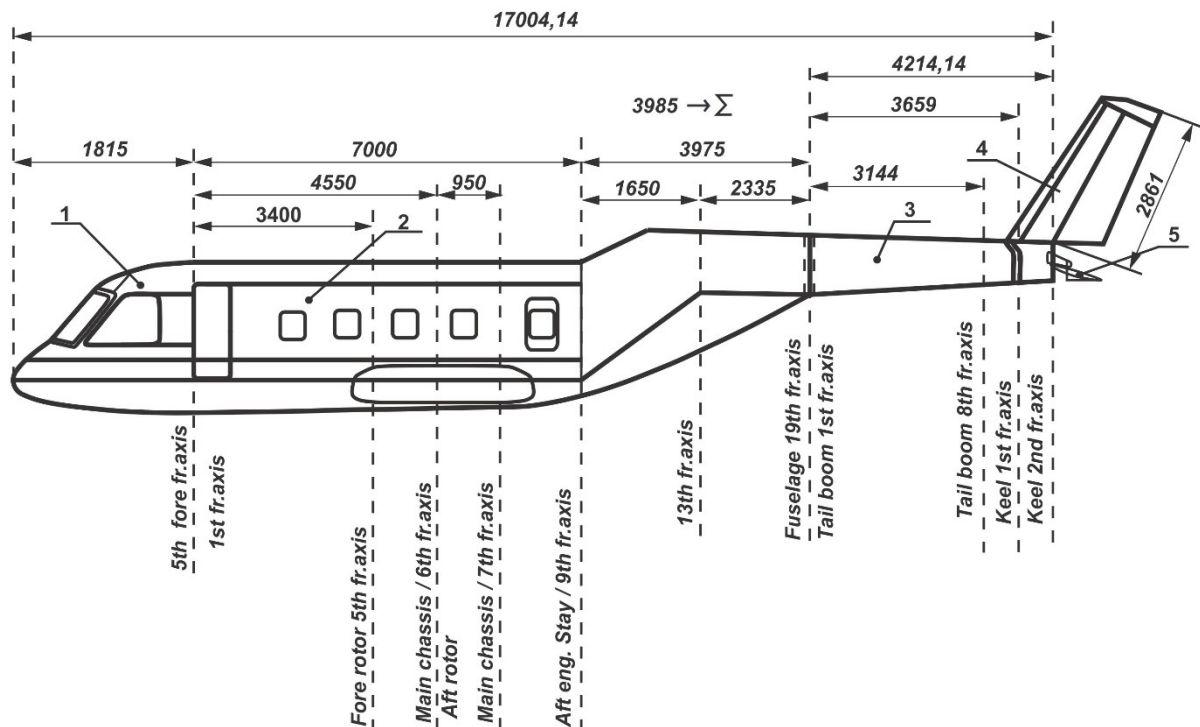


Fig. 2.3. Helicopter fuselage structure.

Fuselage plating consists of a streamlined shape and protects the internal elements of the fuselage against the environmental impact. It withstands local aerodynamic loads, skin deflects loads to the strength stringers and frames.

2.3 Experimental sample bench testing and procedure methodology

2.3.1 Methodology of an experiment for the aluminum alloy samples bench testing

Tests were made using *INSTRON 5500 Series*.

The sample test procedure (Fig. 2.4.) and limiting factors were as follows:

- the samples were loaded up to the collapse;
- each sample was subject to a 5-kN load.

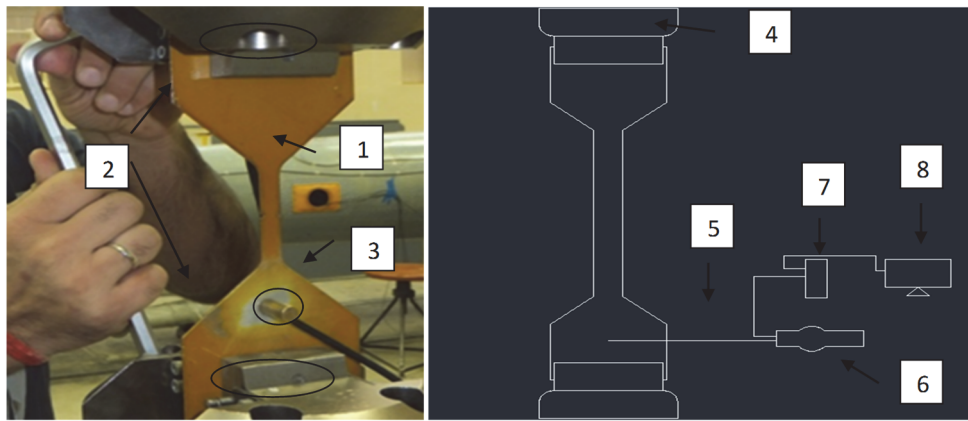


Fig. 2.4. Location of AE sensors on a sample, and sample test scheme [56, 61]:

1 – sample; 2 – clamps; 3 – AE sensor or receiver; 4 – hydraulic cylinder; 5 – sensor cable; 6 – portable equipment PAC Pocket AE2; 7 – computer control unit; 8 – computer screen.

2.3.2 Methodology of an experiment for bench testing of composite material samples

The methods of specimens' testing for determining the mechanical properties stipulated their loading on the following programmes [49, 50]:

- loading up to a failure, without training with the longitudinal direction of fibres (Fig. 2.5) and the transverse direction of the fibres;
- preliminary three-time training to a value of 10 kN or 22 kN for specimens with a longitudinal direction of the fibres and up to 5 kN for specimens with a transverse direction of the fibres, with a subsequent increase in load up to a failure;
- preliminary six-time training to a value of 6 kN (Fig. 2.5.b), with a subsequent increase in load up to a failure for specimens with a longitudinal direction of the fibres.

The experiments were carried out in the thermostatical bench.

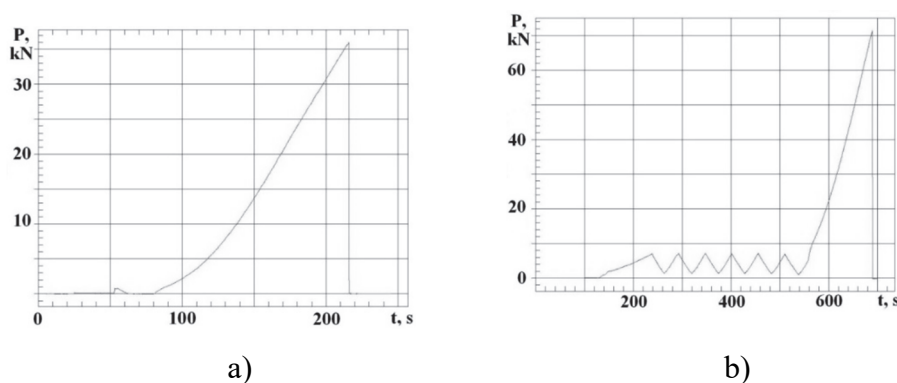


Fig. 2.5. The schedule of loading the specimen with longitudinal arrangement [49]:

a) fibres without training; b) fibres with six-time training.

2.3.3 Methodology of fractographical research

The scanning electron microscope *SEM HITACHI-S3000N* was used to carry out fractographical research during the experiments. The scanning electron microscope is envisaged for research of arigid body surface by means of electrone sound. Fractographical research was based on the methodology developed in [65, 74].

The microscope allows determining the fatigue mesoline nature and its sizes with high precision as well as investigating other crack areas.

2.4 Helicopter structure bench testing methodology and equipment

Helicopter test bench in the laboratory “*Aviatest LNK*” was used to develop a defect localization methodology for technical diagnostics of the helicopter structure fatigue damage. The test object controlled structures and parts thereof:

- 1) helicopter tail boom as a part of helicopter structure;
- 2) helicopter keel as a part of helicopter structure.

Test bench [91] is attached to the strengthened floor, using the chassis power structures (Fig. 2.6).

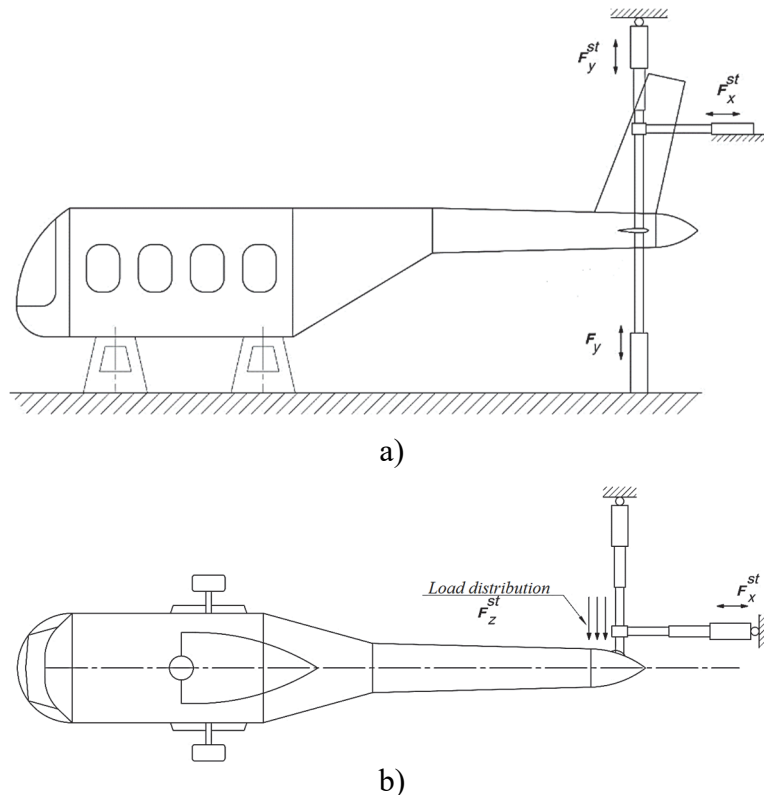


Fig. 2.6. Helicopter structure fatigue test bench:

a) view from the left side; b) view from above.

Test bench is equipped with a special system that allows applying the static load (Fig. 2.7.).

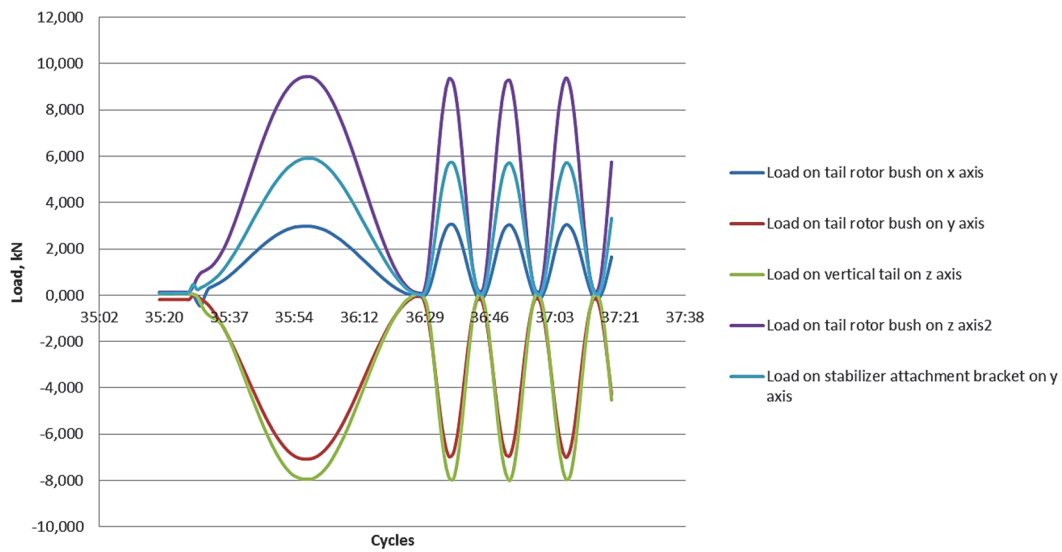


Fig. 2.7. Applied load for a helicopter's structure in time. Start cycle – 60 seconds; ordinary cycle – 15 seconds.

The tests are performed sequentially re-adjusting the static load in order that object stress-strain state complies with the established flight test time (air-ground-air). Maximum flight time loads were recorded at the maximum take-off weight. The load is applied at the hub of helm rotor – F_x^H F_y^H F_z^H , at the fastening points of the stabilizer – F_y as in Fig. 2.8.

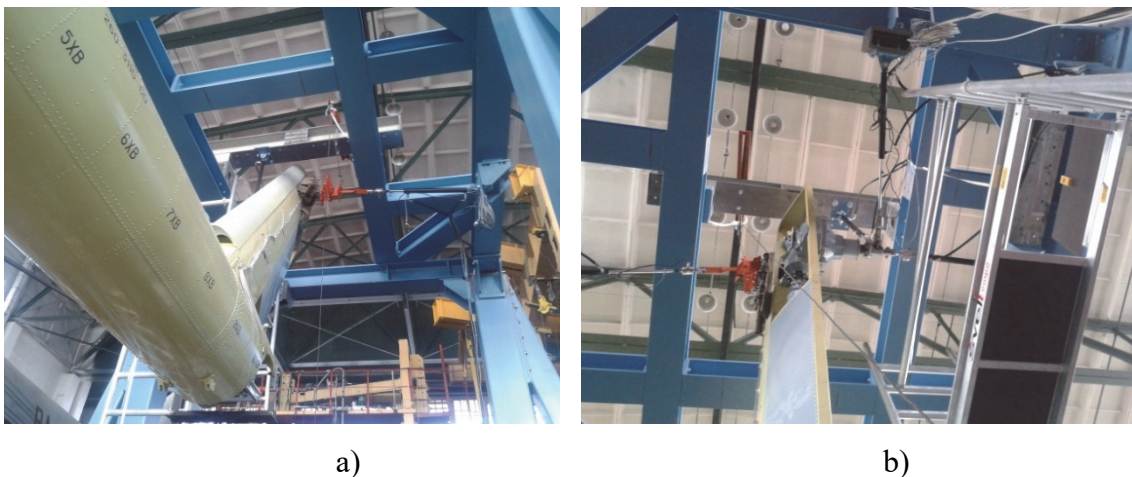
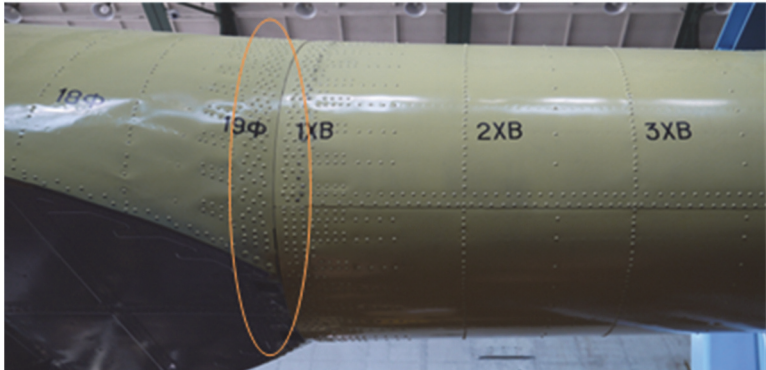


Fig. 2.8. Applied distribution load on the keel for real construction [91]:
a) view against the flying direction from the left side; b) view in the flying direction from the left side.

During the bench tests for crack, fracture and other defects, the following parameters were registered: number of loading cycles, load size, object dimensions, and precise defect location on

the object. During the bench tests for crack, fracture and other defects, the following actions were performed: detected defect was photographed, and an analysis was carried out using fractographic research. In tail boom and keel, the following areas are the most critical points from the fatigue strength point of view:

- a) joint area of the sloping frame No. 13 (Fig. 2.9.c);
- b) joint of tail boom and central fuselage part (Fig. 2.9.a);
- c) joint of tail boom and keel (Fig. 2.9.b).



a)



b)



c)

Fig. 2.9. Tail boom and keel – the most critical points from the fatigue strength point of view:

- a) joint of tail boom and central fuselage part; b) joint of tail boom and keel;
- c) joint area of the sloping frame by frame No. 13.

Acoustic emission sensors on the helicopter structure were deployed as follows:

- *R15α* sensors were installed on the skin of tail boom and keel from the outside (Fig. 2.10);
- *VS-150 RIC* sensors with an internal amplifier were installed on the tail boom frame No. 1 from the inside (Fig. 2.10).

A detailed deployment scheme of AE sensors is shown in the Doctoral Thesis.

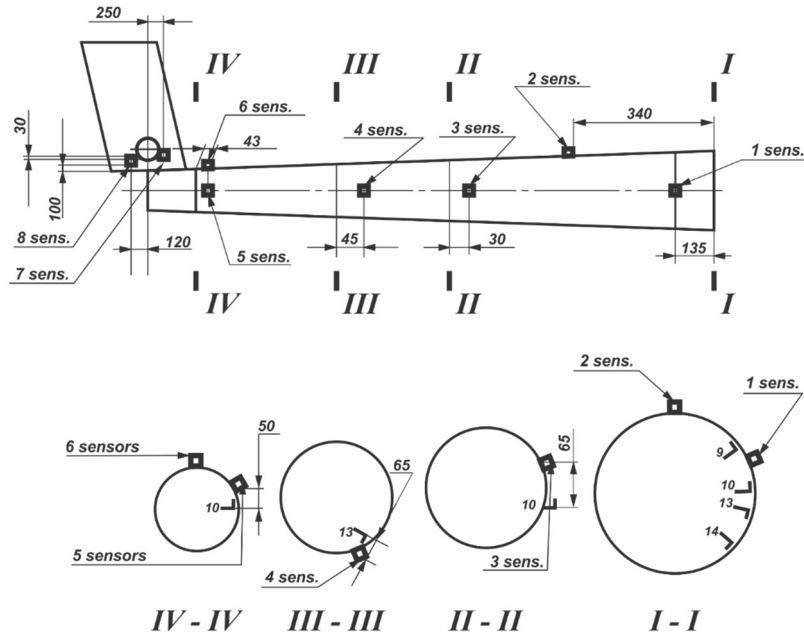


Fig. 2.10. Location of AE sensors on tail boom and keel [55, 57, 59, 62].

3. MATHEMATICAL MODEL OF FATIGUE DEFECT LOCALIZATION FOR MATERIALS AND STRUCTURES

3.1 Defect localization on the plane based on time difference of signal arrival

The most common AE source localization is performed by a signal arrival-time difference method, where the signal arrival time is determined by the maximum amplitude or reaching a threshold.

In cases when the material is anisotropic, defect localization becomes more difficult [19, 20, 66, 68] because the oscillation propagation speed becomes dependent on the direction defined by angle θ . This can be illustrated by the following equation:

$$\Delta t_{1,2} = t_2 - t_1 = \frac{d_2}{v_2} - \frac{d_1}{v_1} = \frac{\sqrt{(x-x_2)^2+(y-y_2)^2}}{v_2} - \frac{\sqrt{(x-x_1)^2+(y-y_1)^2}}{v_1}, \quad (3.1)$$

where d_i – distance to the sensor i ;

v_i – speed of ultrasound in a particular direction with the direction vector

$$\tan(\theta_i) = \frac{(y-y_i)}{(x-x_i)}. \quad (3.2)$$

Thus, it is necessary to have three AE sensors in order to determine the AE source coordinates on the plane; however, in practice, four or more AE sensors are often used to reduce

methodological errors of the coordinates [66, 67]. Equilateral triangle-centred scheme [66, 70] is more often used for AE sensor placement.

Zone detection method [66, 70] is based on the principle that a AE sensor that has registered the highest signal power or amplitude value is the closest to the AE source.

The coordinate calculation error is determined by the time difference of signal arrival (TDOA) measurement errors. There may be many sources of error, for example [66]:

- improper determination of sound propagation speed in the object;
- incorrect determination of the coordinates of the AE sensor, which is a laborious process. One of the possible ways to prevent these errors is the automation of the coordinates of the AE sensor;
- time interval error that depends on the signal structure, its forefront growth in nature, noise level, etc.;
- actual propagation path mismatch [16, 66];
- signal propagation velocity anisotropy existence;
- changes in signal shape during spreading in a structure;
- signal overlapping, as well as multi-source simultaneous operation;
- registration of different types of waves, which spread at different speeds, with AE sensors.

3.2 Mathematical model for fatigue defect localization in aviation structures based on AE signal amplitude

As mentioned before, the defect coordination detection by means of AE is widely used based on TDOA.

It is proposed to use the method of amplitude distribution analysis of AE signals for different groups of AE sensors to solve the problem of determining the coordinates of the defects such as fatigue cracks in these structures.

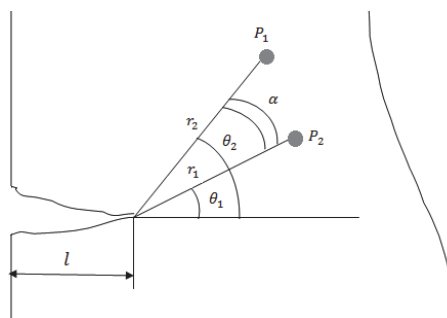


Fig. 3.1. Acoustic emission direction during crack growth [58].

The elementary process of crack growth is increase in its length l by a small value dl (Fig. 3.1). This process is accompanied by the emission of AE signal of sufficiently high amplitude. Impulse amplitude evaluation is done using the ratio that allows determining the movement of the material particles in the vicinity of a crack in a generalized form (3.3), (3.4) [58]:

$$\delta_{ijn} = \frac{k_j}{J} \sqrt{\frac{r}{2\pi}} \varphi_{ijn}(\theta, \mu, r), \quad (3.3)$$

where K_j – tension intensity factor;

r, θ – polar coordinates of a considered point relative to the crack summit;

$$K_j = p_j \sqrt{\pi} Y_j(\lambda), \quad (3.4)$$

where

$\varphi_{ijn}(\theta, \mu, \bar{r})$ – dimensionless function of the angle;

μ – Poisson's ratio;

$\bar{r} = \frac{r}{h}$ – the relative coordinate;

h – thickness of the structure shell with a crack;

J – Young's modulus;

p_j – external specific load component corresponding to the crack type;

$Y_j(\lambda)$ – dimensionless correction function of the relative crack length;

$\lambda = \frac{l}{L}$ – ratio of the absolute length of the crack l to the typical size of the structure

L (length or width depending on orientation of the crack).

Function $Y_j(\lambda)$ depends on several factors [58]:

- the type of a crack;
- configuration and orientation of a crack relative to the coordinate axes;
- geometric parameters of the object;
- characteristics of the loading etc.

Assuming that the amplitude of AE signals is proportional to the corresponding increment of the displacement near the crack summit, $A_{ijn} \cong \delta_{ijn}$.

Due to the known fact directivity of acoustic emission from surges of cracks in the material under other equal conditions, the amplitude of AE signals A_{ijn} depends on the angular coordinate θ . If the acoustic characteristics of the controlled object do not affect this property, it can be defined as the coordinate of the crack and its orientation. Let us assume that the coordinates of the summit of the crack were found through a system of stationary-spaced receiving transducers

or sensors. Then two of them, $P1$ and $P2$, of the known distance r_1 and r_2 to the top of the crack and the angle α characterize the directional diagram of the acoustic emission from the crack (see Fig. 3.1). With exponential nature of the AE signal attenuation, orientation of the crack, for example, with respect to the line OP_1 , characterized by the angle θ_1 , can be determined from the results of the registration of the amplitudes A_{ijn1} and A_{ijn2} registered by transducers or sensors – respectively $P1$ and $P2$ (3.5) [58]:

$$\frac{A_{ijn1}}{A_{ijn2}} = \frac{\varphi_{ijn}(\theta_1, \mu)}{\varphi_{ijn}(\theta_1 + \alpha, \mu)} e^{-k(r_1 - r_2)} . \quad (3.5)$$

Taking into account the AE signal amplitude threshold, the limited signal propagation radius and the limited step of AE changes for real construction diagnostics, the following can be considered: in research areas, AE signal amplitude attenuation has linear character (Fig. 3.2), where angle α describes the slope of the AE signal attenuation curve.

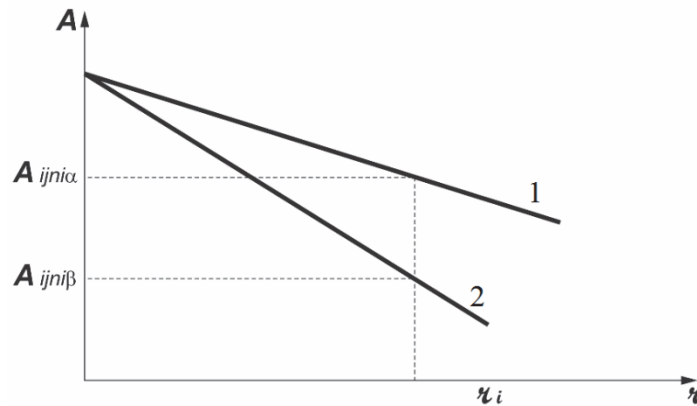


Fig. 3.2. Linear approximate curve of AE signal attenuation.

In the first case when signal propagates in the environment and is registered by two AE sensors, the AE source location is characterized by the radii r_1 and r_2 (3.6 and 3.7) [57, 60, 98]:

$$r_1 = (A_{max} - A_{ijn1}) \cdot \tan \alpha , \quad (3.6)$$

$$r_2 = (A_{max} - A_{ijn2}) \cdot \tan \alpha , \quad (3.7)$$

where A_{max} – maximum amplitude of AE signal in a close proximity to AE sensor;

$A_{ijn1,2}$ – AE signal amplitude values from AE source to the AE sensors No. 1 and No. 2.

It is assumed (Fig. 3.3) that the AE source is located in cluster, described by square, its centre is $P(X_p, Y_p)$, and one side is m . The centre of this cluster is in distance $PD_1 = r_1$ from the AE sensor No. 1 and in distance $PD_2 = r_2$ from the AE sensor No. 2. A square is chosen for cluster

depiction because of aircraft structural elements (rectangular form areas between stringers and frames) and their rectangular characteristics (see Chapter 5.1).

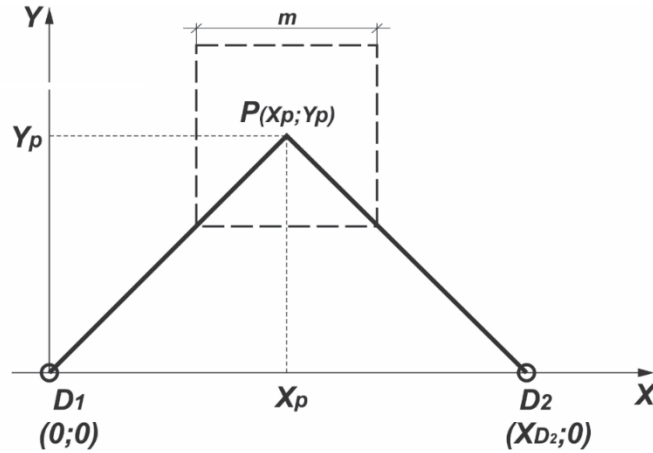


Fig. 3.3. AE source location in cluster with P as a centre.

In a general situation, $\tan \alpha$ characterizes the attenuation curve of AE signal amplitude in a construction material that doesn't have a framing:

$$\tan \beta = \frac{r_i}{A_{max} - A_{ijn1\beta}}, \quad (3.8)$$

then

$$\tan \beta = K_{konstr} \tan \alpha. \quad (3.9)$$

It is possible to find the coordinates X_p and Y_p of the cluster centre P and obtain a coefficient when two AE sensors are located symmetrically to structural elements [57, 60, 98]:

$$X_p = \frac{(A_{ijn2} - A_{ijn1})(2A_{max} - A_{ijn1} - A_{ijn2}) + K_{konstr}^2 \tan^2 \alpha + X_{D2}^2}{2X_{D2}}, \quad (3.10)$$

$$Y_p = \sqrt{(A_{max} - A_{ijn1})^2 K_{konstr}^2 \tan^2 \alpha - \left(\frac{(A_{ijn2} - A_{ijn1})(2A_{max} - A_{ijn1} - A_{ijn2}) + X_{D2}^2}{2X_{D2}} \right)^2}. \quad (3.11)$$

4. EXPERIMENTAL RESEARCH ON AVIATION STRUCTURAL MATERIAL SAMPLES USING ACOUSTIC EMISSION METHOD

4.1 Experimental research on samples made from aluminium alloy under static and dynamic loading

Research of aluminium alloy samples was carried out under static and cyclic loading [56, 61]. The goal of this research was to determine the AE parameters as a criterion for the material

fracture process registration. AE parameters were registered using the AE equipment *PAC Pocket AE-2* and two *KD32* sensors. When applying static load, five samples were tensioned with a maximum load up to their fracture using *INSTRON* equipment.

Analysing the character of the AE signal at the time of the collapse, the following can be concluded – the rapid increase in the amplitude, i.e., for sample No. 3, the amplitude increases from 35...47 dB to 100 dB, and afterwards the collapse successively decreases describing the static breaking moment.

During the dynamic loading test, five samples were used. For the sample No. 2, one loading cycle lasted 0.10 seconds (Fig. 4.1.a), which in total constituted 299 seconds (Fig. 4.1.b), with the variable load from 0.5 kN to 1.5 kN.

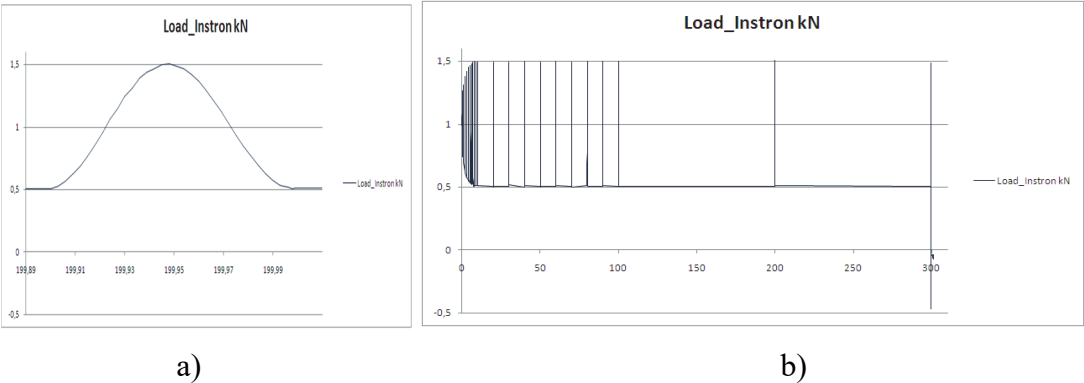


Fig. 4.1. Applied loads for the sample No. 2:
 a – in one load cycle; b – during the entire test.

Such AE signal characteristics as sum count amplitude (Fig. 4.2) and energy reflect the full cycle of all loading. The AE amplitude clearly reflects the collapse moment of the material, when the AE signal amplitude reaches the maximum value from 90 dB to 100 dB, which is characterized by the collapse in the immediate vicinity of the sensor and is obtained from the experiment where samples were loaded with a static load.

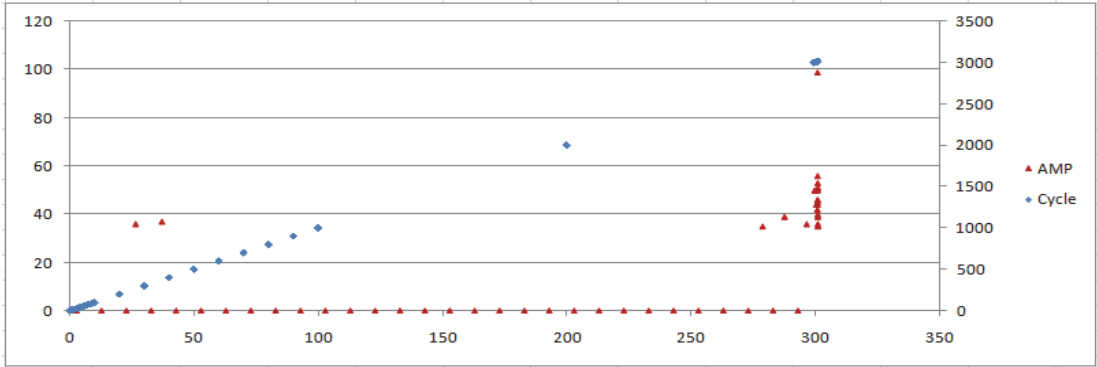


Fig. 4.2. Dependence of the AE signal amplitude on time for the sample No. 2.

4.2 Experimental research on composite material damageability under cyclic loading

Composite material fracture mechanics was analysed using AE method. Tensile tests were carried out on two groups of samples made from fiberglass (Fig. 2) having both warp and weft fibers.

The results are displayed in graphs, where tension and AE parameter – total AE – are compared. The results are obtained under static loading, when tensioned transverse sample had no pre-training (Fig. 4.3.a) [49, 50].

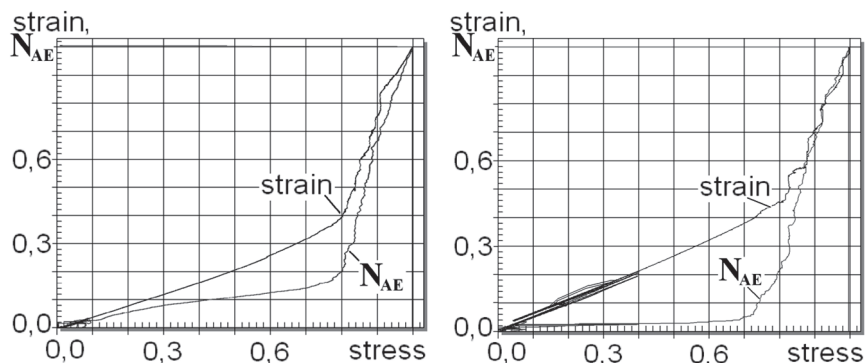


Fig. 4.3. Dependence of the cumulative AE and deformation on the stress-strain of a sample with transverse fibers [49, 50]:

- a) without pre-training (sample width: 20 mm); b) with triple training corresponding to 40% of the breaking load (sample width: 20 mm).

The process depending on the deformation and total AE can be divided into two areas:

- 1) area where the parameters vary proportional to the strain;
- 2) area of intensive growth of the parameters.

The second area describes an irreversible process of a composite fracture, starting from 0.8 of relative strain according to the tension parameter, and from 0.75 according to the AE parameter.

The experiments were carried out to evaluate the effect of pre-training on mechanical characteristics of composite materials; samples were three times pre-trained. It is seen that the whole process is similar to the previous test result (Fig. 4.3.a), i.e., there are areas of the proportional change of deformation parameters and total AE voltage, and the phase of their intensive increment, characterizing, similarly to the first case, the beginning of the process of composite irreversible destruction. However, the beginning of the processes of irreversible damage occurs earlier (starting approximately from 0.7 of the rupture stress by the deformation parameter, and from 0.65 of destructive stress by the parameter of total AE).

All analyzed cases showed preference of AE parameter over tension parameter [49, 50].

When testing composite materials with longitudinal fibre orientation, the experiments were conducted with and without pre-training. Graphical analysis determines three areas of the fracture process [90, 91]:

- 1) the initial stage of total AE intensive growth;
- 2) the stage of total AE stabilization;
- 3) the stage of total AE secondary intensive growth up to destruction.

The character of a composite material sample with longitudinal fibre orientation is shown in Fig. 4.4.

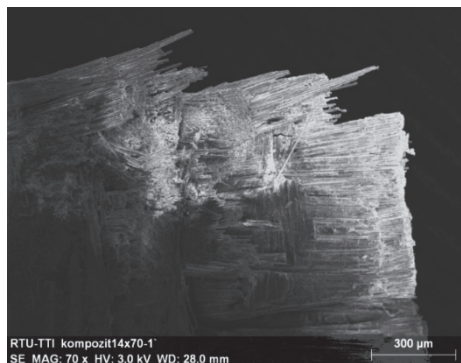


Fig. 4.4. Fragment of a composite material sample with a longitudinal-orientation fracture [49, 50].

Further results [90, 91] of sample testing with training of at least 20% of the ultimate load showed that the S-shaped form remains both with different amounts of training and when the width of the sample is changed, although in these cases the strain measurement, like in the case without training, provides a rectilinear dependence of deformation on stress-strain (Fig. 4.3.b).

Research results [49, 50] allow concluding that pre-training of up to 20% from destruction load does not effect the S-shaped line of total AE, but 2nd and 3rd deformation stages decrease. Further experiments on the samples showed that S-shaped form is dependent neither on the number of pre-trainings nor on the width of the sample. In the same tension, data in all load conditions show constant linear dependance on tension (Fig. 4.3.b).

It is also concluded that three-times pre-training and six-times pre-training are reflected in the total AE S-shaped line as a Caizer effect [33, 50]. In its turn, dependance of total AE does not change. At the same time, when the load exceeds 35% of the burst load, pre-training affects the character of the total AE. Caizer effect still continues to be present, but the dependance of total AE changes sharply. The results suggest that the composite material fracture process is a two-stage process, and it is important that most parts of microfracture processes are allocated to the first process.

5. HELICOPTER STRUCTURE FATIGUE DAMAGE DIAGNOSTICS WITH DEFECT LOCALIZATION

5.1 Analysis of AE signal propagation features in helicopter structural elements

5.1.1 Analysis of AE signal propagation in helicopter skin with framing elements

AE signal amplitude evaluation and signal propagation speed measurements have been made on helicopter skin taking into account such parameters as stringers, frames, and riveted and glued joint influence (Fig. 5.1.a, b) [58, 60].

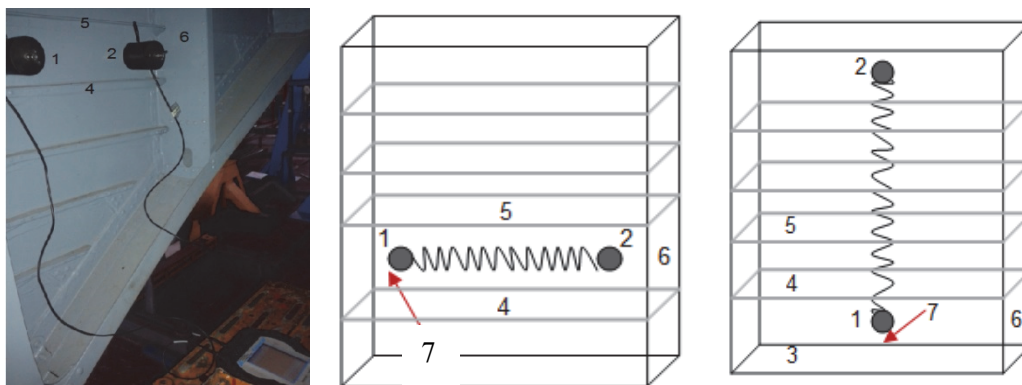


Fig. 5.1. AE sensor displacement on the fuselage for the sound velocity and amplitude attenuation research:

- 1, 2 – AE sensors; 3 – AE source imitation point; 4, 5 – stringers No. 4 and No. 5;
6 – frame No. 10; 7 – AE source imitation point.

Four sensors were simultaneously used for measuring ultrasonic speed and AE signal amplitude attenuation. The measurements of AE signal for sound velocity and AE signal amplitude were simulated by breaking a pencil lead eight times in one point by Hsu-Nielsen method.

1st measurement model

In the first case, AE sensors were placed on the plating (Fig. 5.1.c) between frames No. 9 and No. 10 and stringers No. 4 and No. 5, 248 mm apart from each other, in order to obtain the results of sound velocity and AE signal amplitude attenuation over the plating without framing impact, but still taking into account the material properties and painting of helicopter plating.

2nd measurement model

In the second case, AE sensors were placed on the plating (Fig. 5.1.c) between frames No. 9 and No. 10 and stringers No. 3, No. 4 and No. 7, No. 8, 400 mm apart from each other, in

order to obtain the results of sound velocity and AE signal amplitude attenuation over the plating with stringer impact.

3rd measurement model

In third case, AE sensors were placed in the same manner as in the second case, but AE source imitation point was changed (Fig. 4) in order to obtain the results of sound velocity and AE signal amplitude attenuation over the plating with stringer and frame impact. Helicopter fuselage frames are riveted.

The relative error of the measurements is within the range of 0.63–0.84%.

The characteristics of AE signal are shown in Table 5.1 [58].

Table 5.1

Average signal amplitude to sensors and attenuation of AE signal amplitude in plating during different measurement models

Measurement model No.	Average AE signal amplitude to sensor No.1, [dB]	Average AE signal amplitude to sensor No.2, [dB]	Attenuation of AE signal amplitude in plating, [dB/mm]	Average sound velocity, [m/s]	
1	82.88	70.50	0.050	5141.49	
2	82.78	48.38	0.087	2193.02	
3	3-7	65.58	66.75	0.040	–
	3-8	69.33	67.89	0.030	–
	3-9	68.89	70.78	0.017	–
	3-10	57.27	56.55	0.055	–
	3-11	60.00	54.78	0.042	–
	3-12	58.29	50.00	0.040	–
	3-13	55.73	45.45	0.039	–

The overall conclusion is that the attenuation of AE signal amplitude depends on the AE source angle with respect to the AE sensor, and its reduction is [58]:

- 0.0019 dB/mm at sound imitation points 7, 8, 9 before the frame No. 10 for each 3 degrees of slope;
- 0.0019 dB/mm at sound imitation points 11, 12, 13 after the frame No. 10 for each 3 degrees of slope.

Consequently, the attenuation value depends not only on the distance from the sound point to the AE sensor, but also on its location angle to the sensor – the signal amplitude is considerably larger from the signal point that has steeper angle to the AE sensor.

5.1.2 Attenuation card creation for AE signal amplitude in helicopter fuselage

In order to create the attenuation card for AE signal amplitude in helicopter fuselage, experiments [60] were performed inside the fuselage taking into account the frame – stringers and frames. Four AE sensors were used in the experiment – one sensor was placed on the stringer No. 6 between frames No. 9 and No. 10; one sensor was placed on the stringer No. 10 between frames No. 6 and No. 7; the third and fourth sensor were placed on the fuselage between stringers No. 7 and No. 8 and frames No. 9 and No. 10, from inside and outside respectively.



Fig. 5.2. Location of AE sensors on helicopter fuselage.

During imitating AE signal on the fuselage between frames No. 9 and No. 10, the arrival of signals was registered on all four sensors (Figs 5.3 and 5.4). Highest amplitudes were registered in close proximity of the respective sensors. In overall, lowest amplitudes were noticed on sensors that were placed on the frames. All sensors registered the signals initiated by stringers No. 16 and No. 17, and their amplitude level was above the set threshold of 35 dB [60].

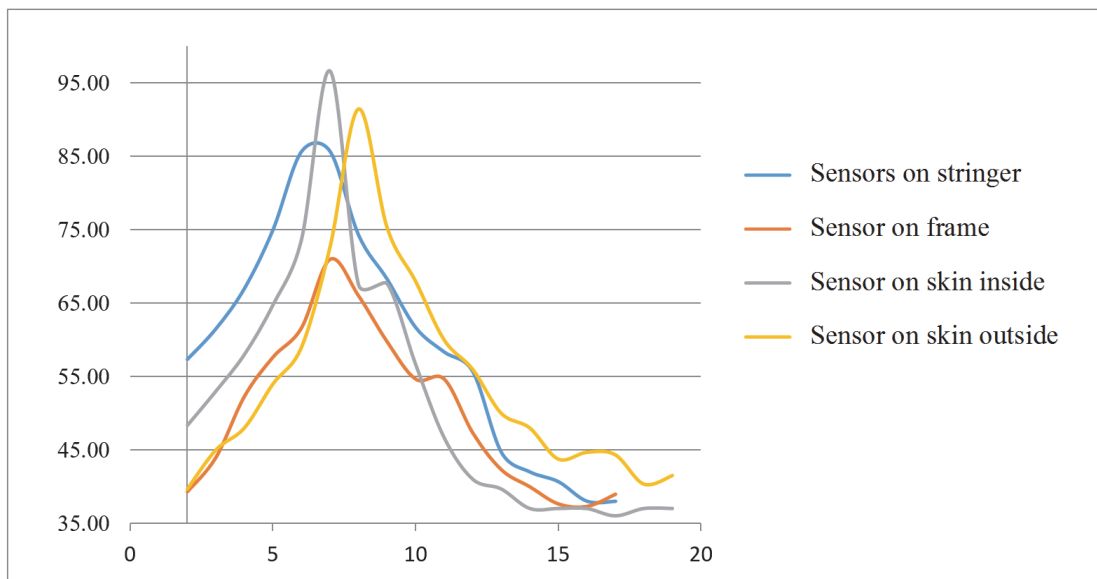


Fig. 5.3. Imitated AE signal amplitude, dB (y axis) on stringers Nos 1–22 (x axis) between frames No. 9 and No. 10.

The charts of AE signal amplitude attenuation were created after summarizing the signal receiving amplitudes (Fig. 5.4). They illustrate the registered AE signal amplitude from the source located in a particular distance; besides, the amplitudes only above the 35-dB threshold were taken into account [60].

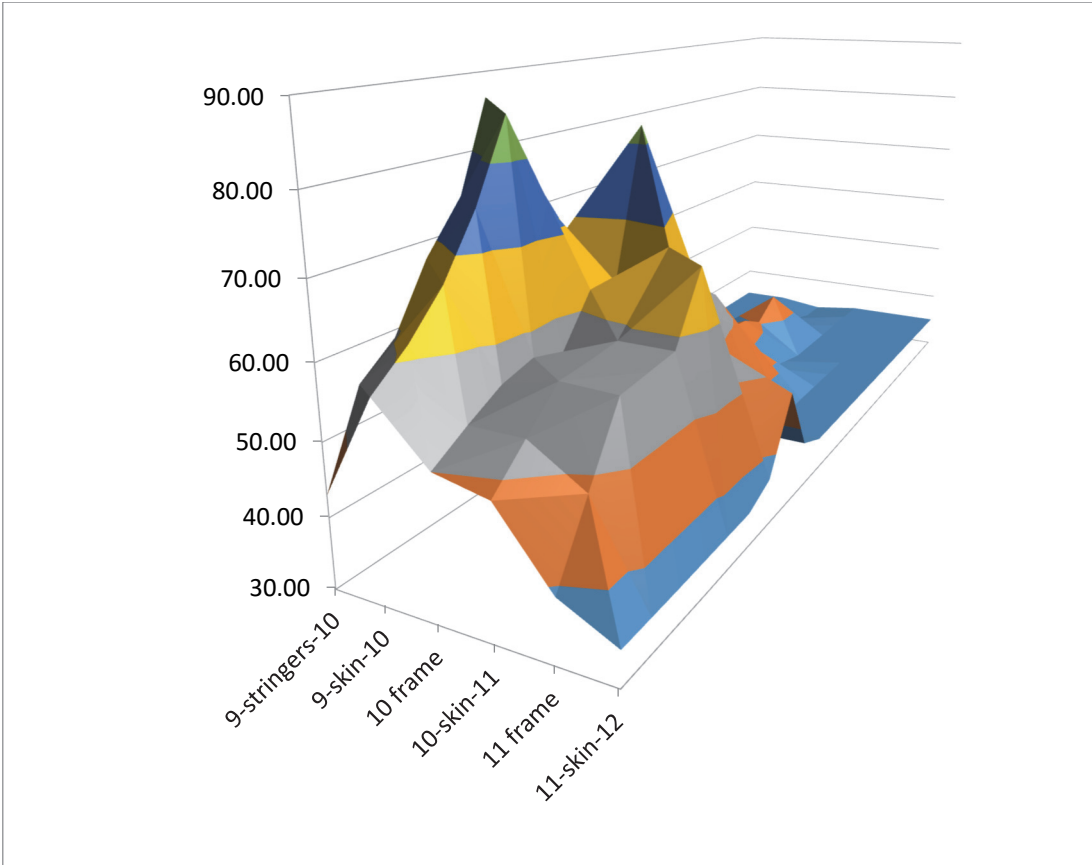


Fig. 5.4. Registration of AE signal amplitude on the sensors placed on stringers.

The results of the experiment when AE sensors were placed on helicopter tail boom and keel were used to create a diagnostic system. A conclusion is that the placement of sensors on the outside of the fuselage is not recommended even when performing test bench experiments.

For control of particular parts of the helicopter structure, the most advisable way of sensor placement is: to place sensors on a particular element, i.e. during frame control, sensors are placed on the frames; to calculate the number of sensors depending on the geometrical parameters of the structural elements and using the obtained charts of AE signal amplitude attenuation.

Taking into account that the above mentioned task for helicopter structure diagnostics is planned to be solved reflexively, i.e., by analysing the value of AE signal amplitude on the sensors to determine the location of defects, the main task of the experimental research was to determine the changes in the intervals of AE signal amplitude taking into account the helicopter structural framing.

5.1.3 Determination of the coefficient of AE signal amplitude changes in helicopter structure for defect localization

An imitation quadrate with a schematic network of 40 cm × 40 cm was created in order to conduct the studies on helicopter plating (from the outside). The square was divided into smaller squares, 5 cm × 5 cm, with the total of 64 imitation points. The quadrate was designed to include both the design of the frames and stringers (one frame (No. 10F) and four stringers) [98].

An AE sensor was placed in each of the corners of the square (Fig. 5.5.a). The signal was imitated 8 to 10 times in the middle of each small square. The results are summarized in a graphic form (Fig. 5.5.b). The relative error is obtained, and the average value of the compiled data is 0.86% to 0.90%.

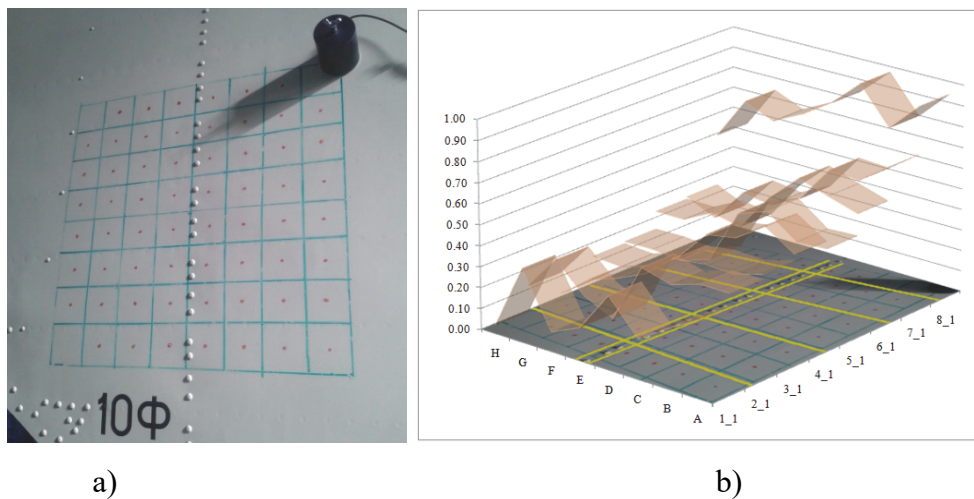


Fig. 5.5. AE signal imitation quadrate:

- a) location of the AE sensor No. 3 in the point No. H1; b) AE signal amplitudes (in relative units) registered on the sensor No. 2 in the point No. A8.

The graph of the dependance of the AE signal amplitude on the location of AE source was approximated by linear approximation.

Analysing AE registration amplitude on sensors, it should be noted that higher amplitude signals are registered from the sources located on the fuselage skin before the framing. Experimentally it is proved that the AE signal amplitude registered on the sensors is smaller if the source is equidistant from the sensor but there is the framing in signal distribution area. It is also proved that the curve slope of the attenuation of AE signal amplitude (according to the AE source location detection by the amplitude theoretical model discussed in Chapter No. 3) depends on the type of framing elements and their amount in the AE signal propagation area. For example, in the case when the AE source is in the area from No. H8 to No. A8, the signal propagation distribution after linear approximation does not exceed 0.039. Thus, according to the expression (5.1) [98]:

$$\tan \alpha_{H8} = 0.875. \quad (5.1)$$

Comparison of the AE signal amplitudes at the same distance r_l from the sensor No. A8 – in squares No. A1 and No. H8 (Fig. 5.6) – shows that they are 0.38 and 0.54 in relative units respectively. In the first case, there are four stringer joints; in the second case, there is one frame joint. Thus (5.2):

$$\tan \alpha_{A1} = 0.614. \quad (5.2)$$

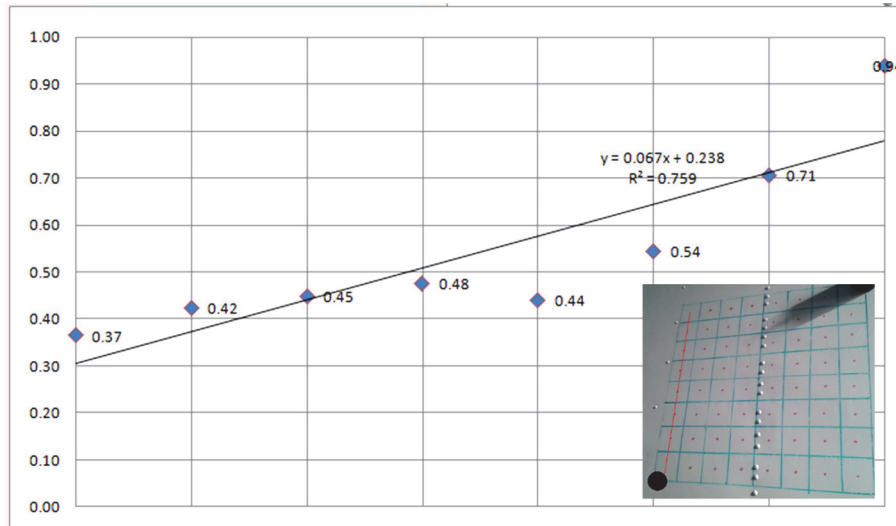


Fig. 5.6. Values of AE signal amplitude (y axis) in squares No. A1 to No. A8 (x axis).

The value $\tan \alpha_{skin}$ was determined experimentally – when helicopter fuselage is without framing at distance $r_1 - \tan \alpha_{skin} = 1.5$. The AE signal amplitude attenuation coefficients are applied in points No. A1 and No. H8 to detect and obtain the location coordinates of defect: $K_{str} = 0.41$ and $K_{br} = 0.58$.

Consequently:

$$r_{H8} = 0.35 \text{ m.}$$

For example, AE source location r_i can be easily calculated if the registered AE signal amplitude $A_{ijni} = 0.84$ and it is known that the signal propagates in the area zone with the stringer framing (5.3):

$$r_i = (A_{max} - A_{ijni}) \cdot K_{str} \cdot \tan \alpha_{ap\check{s}}. \quad (5.3)$$

Thus, $r_i = 0,28 \text{ m}$, which corresponds to the square No. A3.

Overall, it can be concluded that the signal amplitude attenuation coefficient in this research study is within the range of 0.37–0.58.

Summarizing the obtained values of AE signal amplitude, it can be concluded that it is possible to determine location of defects by signal amplitudes using the proposed coefficients. Moreover, it is possible to determine the location of defects by AE signal amplitudes even for such elements that have frames and stringers.

5.2 Diagnostics of bolted joints using the acoustic emission method during helicopter bench tests

The parameters of acoustic emission (AE) signals were measured during the bench tests of the tail boom structure and fin, the joint areas of the fin, and the tail boom and fuselage of the helicopter (the joint area of the 1st and 19th frames of the tail boom and fuselage respectively) [55, 57, 59, 62].

Measurement methodology is given in Chapter 2 of the present Thesis. This chapter describes the defects determined during the experiment. Control of the development of those defects was done using the AE method until fracture or accelerated growth of the crack.

5.2.1 Overall evaluation of the informational content of AE signal diagnostic parameters

On the basis of analysis of AE parameters recorded in the process of testing [55, 57, 59, 62], the following was revealed. The AE signal amplitude (Fig. 5.7) recorded for all channels quantitatively reflects the process of failure. The value of amplitude depends on the point of AE sensor installation including its orientation relative to the source of AE signal and the distance to the source. The energy of AE signals (Fig. 5.8) is also an informative parameter for the diagnostics of large structures; this parameter quantitatively reflects the stages of the process of accelerated crack growth in the material of helicopter structural components. Due to significant influence of mechanical noises during the tests, total AE is only informative in the case of additional filtration. This process is rather time-consuming and requires the development and application of a special program for the processing of recorded signals.

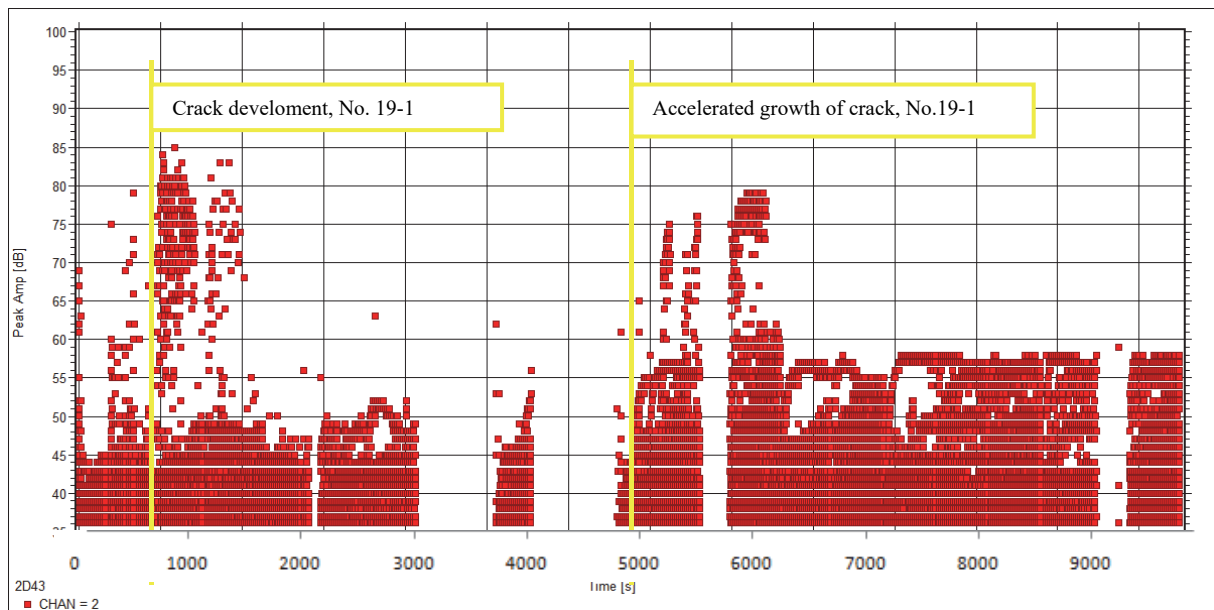


Fig. 5.7. The amplitude of AE signals, and dB (y axis) recorded in the interval of 1-9812 load cycles (x axis).

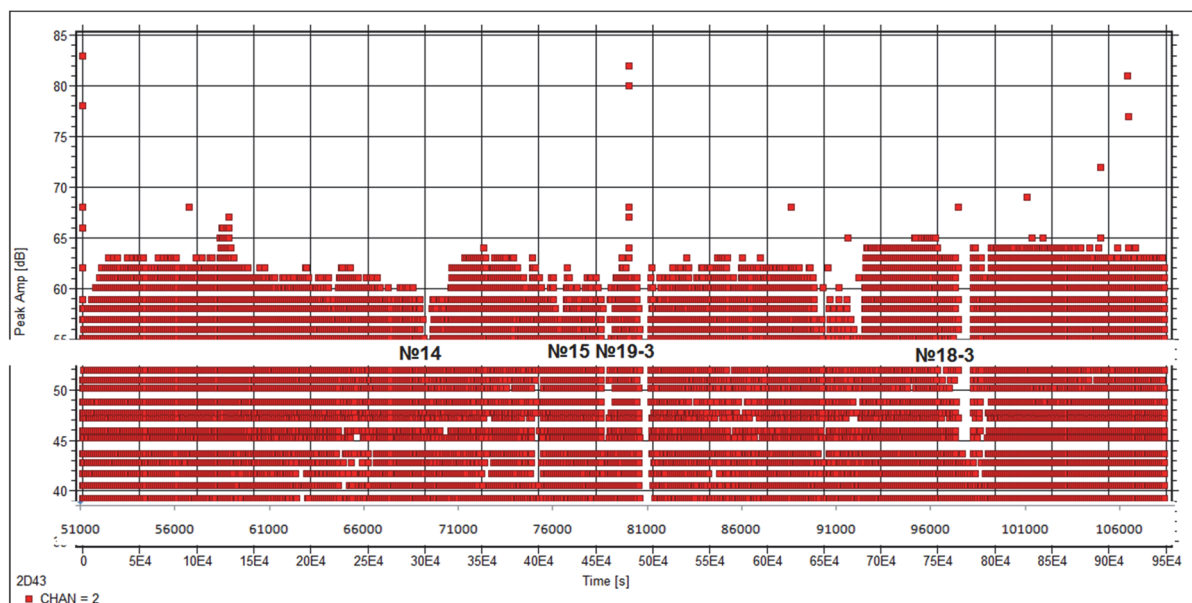


Fig. 5.8. The amplitude of AE signals, and dB (y axis) recorded in the interval of 51000-108958 load cycles (x axis).

5.2.2 General characteristics of the results of fractal analysis of bolt material fractures

On the basis of the fractal analysis we carried out, it was found that the propagation of fractures in bolt material is characterized by the formation of low-cycle fatigue damage mesolines (Fig. 5.10.a), the distance among which increases in a general case, which characterizes the acceleration of crack growth rate as the crack length increases (fatigue damage areas). In all cases, the failure has a multinuclear nature (Fig. 5.9). The material of bolts contains inclusions (Fig. 5.10.b) [55, 57, 59, 62].

At the same time, the failure of bolts has a complex nature due to the influence of additional factors:

- cracks initiate and grow simultaneously in several bolts leading to the redistribution of load among them right during the tests, which is reflected in the mechanism of crack propagation;
- after periodic retightening of bolts during the tests (some bolts were retightened up to three times), the redistribution of stresses causes changes in the nature of fatigue mesoline propagation – their obvious transition from small to larger size along with the propagation of damage was not observed.

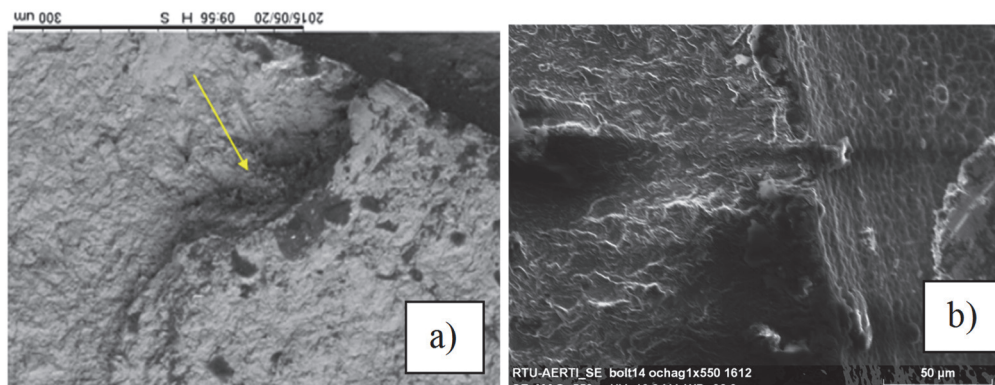


Fig. 5.9. Nucleus area: a) No. 19; b) No. 14.

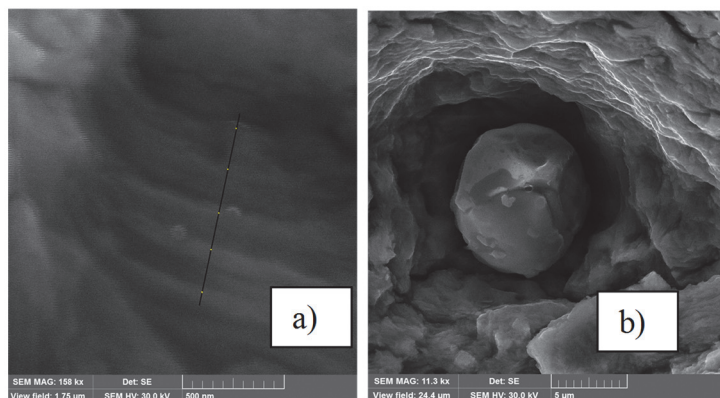


Fig. 5.10. Bolt No. 19-1: a) fatigue mesoline, $h = 0.15\text{--}0.17\ \mu\text{m}$; b) inclusion.

5.2.3 Individual evaluation of the results of acoustic emission diagnostics of bolts in the joint between the tail boom and fuselage during helicopter structure life tests

Analysis of test results [95, 96] before the failure of bolts No. 19-1 and No. 18-1

On the basis of AE monitoring data, in the process of inspection of 23022 load cycles, it was found that attachment bolts No. 19-1 and No. 18-1 in the area of stringers 5 and 6 along the right side had failed (Fig. 5.11).

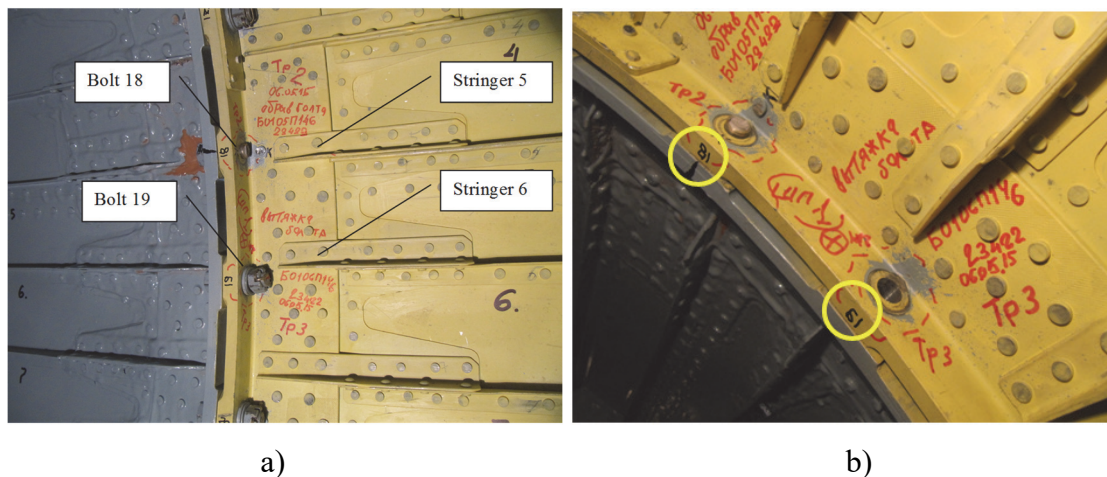


Fig. 5.11. General view of the failed bolts No. 19-1 and No. 18-1:

a) general view of the area of fuselage and tail boom joint; b) view of the holes for the bolts 18-1 and 19-1.

The fractures of both bolts have a fatigue nature (Fig. 5.12).

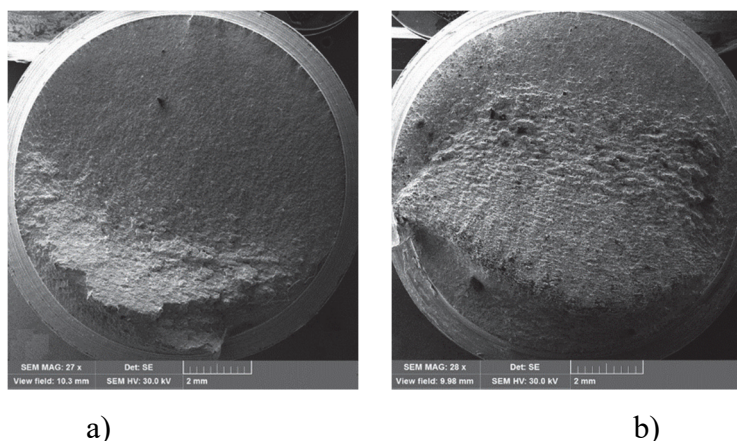


Fig. 5.12. Fatigue fractures of bolts:

a) fracture of the bolt No. 19-1; b) fracture of the bolt No. 18-1.

The relief of the fracture of bolt No. 19-1 is characterized by higher fineness. This is indicative of a relatively low crack growth rate and corresponding duration of destruction process. The nucleus area of the crack is a base of the 1st thread turn profile (Fig. 5.12.a). The relative area of fracture fatigue zone is approx. 80%.

The relief of the fracture of bolt No. 18-1 for stringer 5 is characterized by coarse granulation (Fig. 5.12.b), which is an evidence of a higher crack propagation rate. The relative area of the bolt fracture fatigue zone is markedly smaller, which is also an indicative of an increased crack propagation rate. In this case, the base of the thread profile is also a nucleus area of the crack.

The distribution of fracture relief and fatigue zone relative areas among the bolts allows considering that originally the crack appeared in the material of bolt No. 19-1. The analysis of the

curves of AE parameter records reveals the presence of several more nuclei of fatigue damage, in particular, accelerated fatigue crack growth was detected in the interval from 15400...15600 to 17600...17800 load cycles, which probably reflects the kinetics of fatigue crack propagation in the material of bolt No. 18-1 (Fig. 5.13).

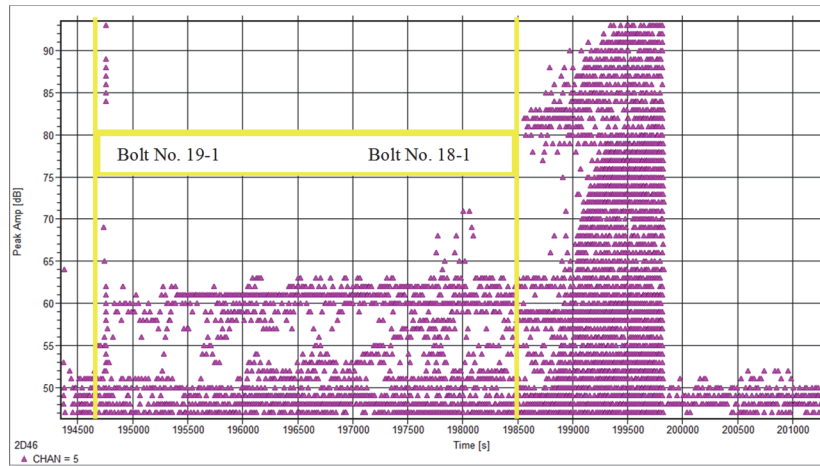


Fig. 5.13. Time-dependent behaviour of AE signal amplitude, dB (y axis) from 9812 load cycles to the failure, bolts No. 18-1 and No. 19-1 (x axis).

According to the results of our fractographic examination, in the case of bolt No. 19, the crack growth rate at the initial stage of destruction was on average $0.08\text{--}0.09\ \mu\text{m}/\text{cycle}$. This regularity was being observed until the crack reached a length of approx. $260\ \mu\text{m}$, which corresponds to 3000...4000 load cycles. Then the changes in crack growth rate were detected at the levels of $0.15\ \mu\text{m}/\text{cycle}$ and $0.25\text{--}0.35\ \mu\text{m}/\text{cycle}$ (Fig. 5.14). The specified rate was being observed up to the bolt failure at approx. 18000...19000 load cycles. The propagation of the crack in the material of bolt No. 18 also occurred with an average rate of $0.25\text{--}0.35\ \mu\text{m}/\text{cycle}$, which corresponds to approx. 6000...7000 load cycles. In the area of accelerated crack growth, it is possible to observe some characteristic zones of sliding.

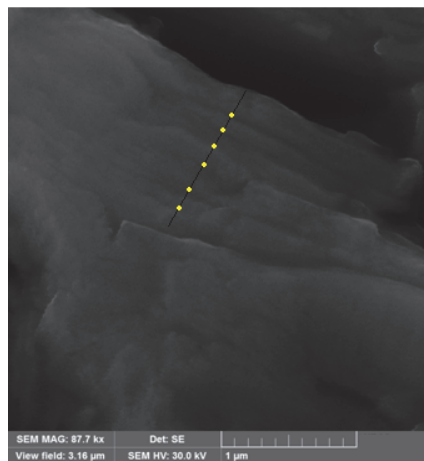


Fig. 5.14. Fatigue mesolines, $h = 0.11\text{--}0.16\ \mu\text{m}$, bolt No. 19.

Analysis of test results before the failure of bolts No. 19-2 and No. 18-2

The tests were continued after the replacement of failed attachment bolts No. 18-1 and No. 19-1 in the area of stringers 5 and 6 along the right side of the tail boom in 23022 load cycles with new bolts numbered 18-2 and 19-2 respectively. The tests were accompanied by continuous recording of AE signals on all selected channels up to 51000 load cycles when during a regular inspection a repeated failure of bolts 18 and 19 was revealed. The total operating time of bolts from the moment of their installation to their complete failure was 27978 cycles. On the basis of AE measurements, which are common for both bolts, the accelerated growth of fatigue cracks was detected at 46600–47000 load cycles (Fig. 5.15).

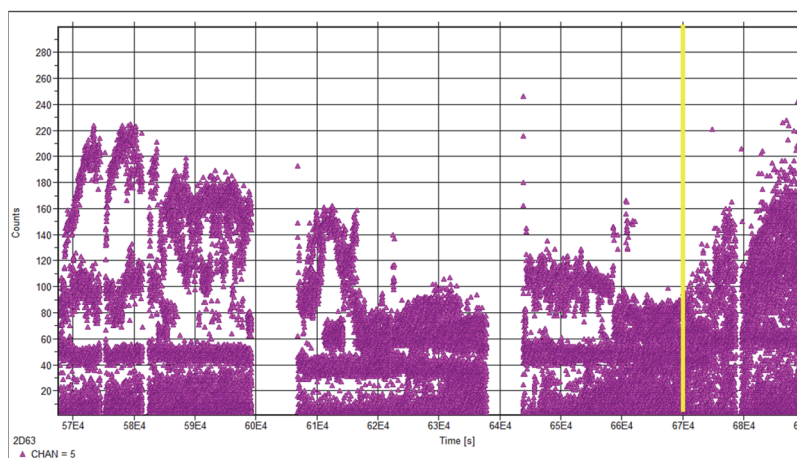


Fig. 5.15. Time-dependent behaviour of the AE signal intensity.

The nature and dimensions of corresponding fatigue fracture zones of the bolts are in many ways similar to the fractures of the bolts previously failed at the same place. Based on the analysis of distribution of fracture relief and fatigue zone relative areas in bolt section, it was found that the initial crack appeared in bolt No. 19. Here the base of the first (from the cylindrical part of the bolt) thread profile is also a nucleus zone of the cracks.

Analysis of test results before the failure of bolt No. 19-3

After the completion of another stage of tests in 80 615 load cycles, the inspection helped to reveal the 3rd (during the tests) failure of the attachment bolt for the hole No. 19 in the area of stringer 6 along the right side. The fracture (Fig. 5.16) has a fatigue nature typical for all the previously failed attachment bolts. The fatigue zone occupies about 95% of its area and consists of a fine-grained site (more than 60% of fracture area) and a coarse-grained site.



Fig. 5.16. Fracture of bolt No. 19-3 on the bolt shank.

The failure of bolt No. 19-3 was detected by all the AE sensors installed in the area of tail boom and fuselage joint. The failure of this bolt is characterized by AE signals with an amplitude increasing up to 80...85 dB (Fig. 5.17.) at the 80050...80100 load cycle. At the same time, the accelerated growth of the crack in the bolt material was detected after reaching the 78800...78900 load cycle when AE signal amplitudes increased up to 60...62 dB. The accelerated growth of the crack was being observed during about 1250 cycles, i.e., in the case of applying the AE method during operation, the bolt failure could be predicted approx. 26 flying hours ahead.

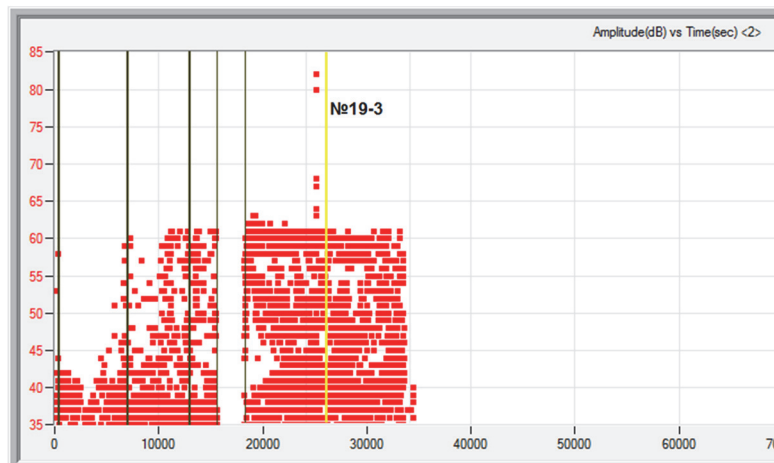


Fig. 5.17. Time-dependent behaviour of AE signal amplitude (y axis) during the accelerated growth of the crack until the fracture, bolt No. 19-3.

The analysis of AE signal energy behaviour during the accelerated growth of the crack in the material of bolt No. 19-3 revealed the moment the crucial crack growth began (430–435 cycles before the failure). Further fractal analysis of the fracture showed the correspondence of this loading period to the rupture area. The crucial growth of the crack corresponds to approx. 8

estimated flying hours. In the material of bolt No. 19, the range of fatigue mesoline dimensions in the area on a radius of up to 500 μm from the nucleus is 112–134 nm/cycle. The length of the given site corresponds to 4065 load cycles.

The subsequent 500 μm the crack was propagating at a rate of 125–142 nm/cycle. The length of the given site corresponds to 3759 load cycles. Then the next 2000 μm the crack was propagating during 12345 c at an average rate of 162 nm/cycle. The total life at this stage corresponds to 20169 load cycles. Then, on a radius of about 3000 μm from the nucleus the slower growth of the crack was observed (Fig. 5.18). This site corresponds to the moment of bolt retightening (twice) after the failure of bolts 14 and 15 in 69603 and 78601 load cycles respectively. The length of this site corresponded to 10 447 load cycles. Then, for approx. 1000–1500 μm , there continued a slower growth of the crack at a rate of 90–110 nm/cycle, which corresponds to 9197 load cycles.

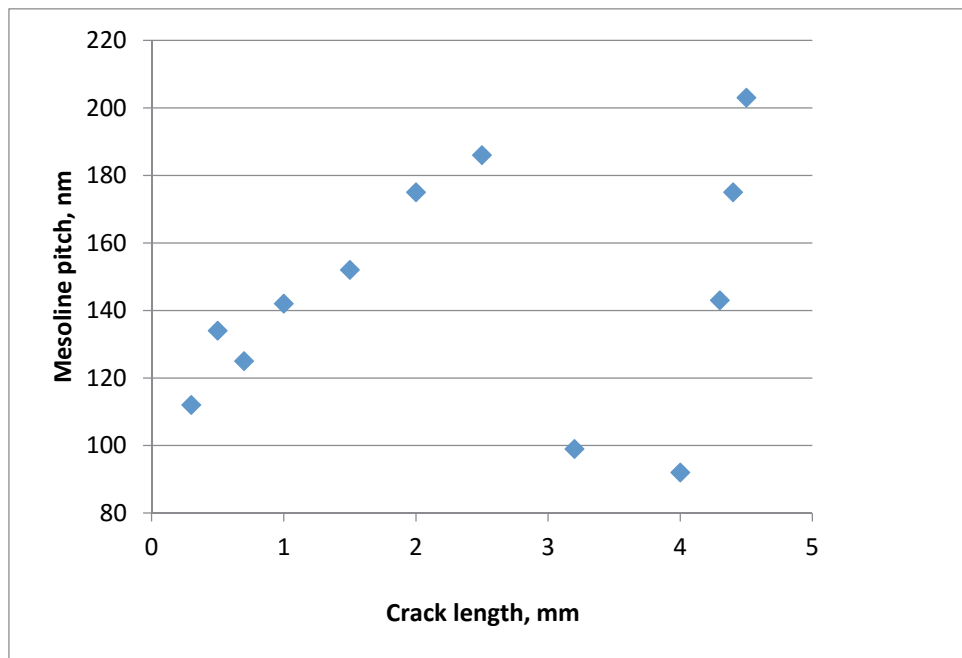


Fig. 5.18. Dependence of fatigue striation increment on the length of the fatigue crack with account of retightening of bolts in the joint between the tail boom and fuselage, bolt No. 19-3.

After that, the crack growth accelerated up to the rate of 200 nm/cycle. On a radius of about 4–4.5 mm (Fig. 5.19) from the nucleus area, the failure has a mixed nature reflecting the accelerated growth of the crack. The total life of the bolt material is 30 616 load cycles.

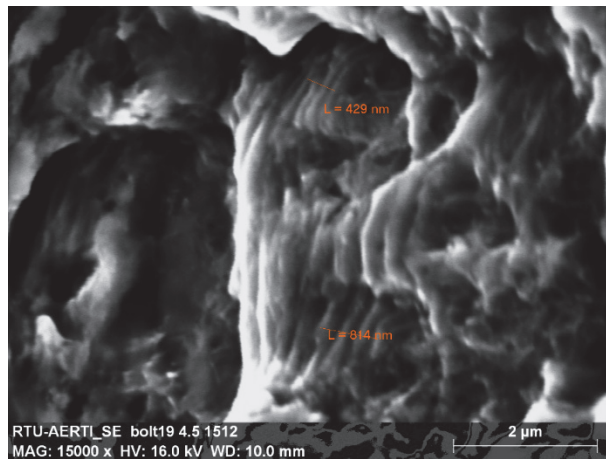


Fig. 5.19. Fatigue mesolines, $h = 143..203$ nm/cycle (4.5 mm from the nucleus).

5.3 Evaluation of the defects of riveted connections

5.3.1 The AE control methodology of the technical condition of riveted connections

The application of the classic AE method for monitoring the condition of bolted and riveted connections during operation is very limited. The necessity to apply a load to connection components, which initiates defect development, in its turn, by the generation of ultrasonic signals, is a mandatory requirement of AE monitoring. Monitoring of connections without any load is not possible yet.

The method used in this research also implies recording of signals and analysis of AE method when monitoring the condition of riveted connections parameters. However, in such a case, the ultrasonic signals generated by the AE source simulator set on one of the parts being connected (rather than the signals initiated by the developing defects of the loaded components) are recorded. In this case, AE signals are received by the AE transducer installed on the head of the rivet being monitored. An option is also possible when ultrasonic signals are generated with the imitator of AE sources installed on the head of the rivet being monitored, while the AE receiver is installed on one of the parts being connected. The condition of the rivet is evaluated on the basis of the results of comparing the intensity level or amplitude of the recorded signal with the level of rejection. The general condition of the connection is evaluated based on the ratio of defective rivets to the total number of rivets in the connection. Thus, the experiment makes it possible to give a quantitative estimation of the condition of both separate components and the bolted or riveted connections as a whole in real conditions of structure operation.

To monitor the condition of riveted connections, the pulsar was placed on the frames near each joint, and the transducer of AE signals was placed on the rivet head. As in accordance with Fig. 5.20, where joint No. 3 is in satisfactory condition and joint No. 6 has the worst corrosion

wear, a comparative evaluation of the condition of riveted connections in joints No. 3 and No. 6 in plates 6, 7 and 8 was carried out. The pulsar was sequentially placed on plates 6, 7 and 8, while the AE sensor was used to respectively receive the signal from the head of each rivet. Fig. 5.20 represents the diagrams containing the numbering of the rivets being monitored and the results of the tests [8, 40].

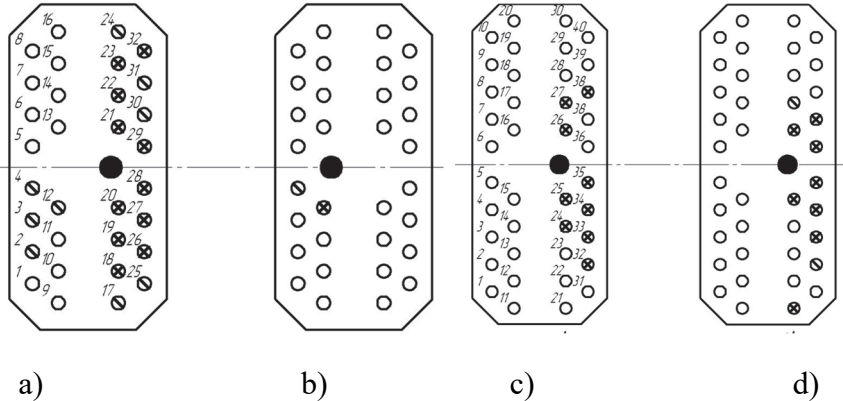


Fig. 5.20. Diagrams of rivet numbering, and results of testing the bottom of the joints No. 3R and No. 6R in various connections:

- a) plate 6, joint No. 3R; b) plate 7, joint No. 3R; c) plate 6, joint No. 6R;
- d) plate 6, joint No. 6R (additional measurement), where ⊗ – non defected rivets; ⊖ – rivets in transient condition; ○ – faulty condition; ● – pulsar location.

When the pulsar was installed on plate 6, the steady signal was received from the rivets Nos 18 (Fig. 6), 19, 20, 21, 22, 23, 26, 27, 28, 29, 32 (Fig. 5.21); the unstable signal was received from the rivets Nos 2, 3, 4, 12 (Fig. 7), 17, 24, 25, 30, 31; no signal was detected on the rest of the rivets (i.e., the AE signal was received from approx. 47% of the total number of rivets). The general evaluation of the condition of the riveted connections for the connection (a) (see Fig. 5.20.a): 47% of the total numbers of rivets in the connection are found to be suitable for further use.

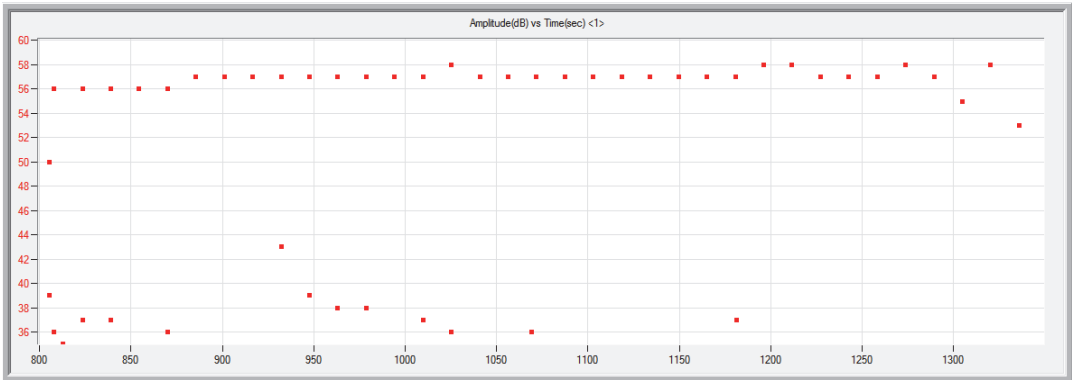


Fig. 5.21. Time-dependent steady AE signal with an amplitude of approx. 57 dB (y axis) received from the rivet No. 18.

The analysis of AE signal passage along the above AE path according to the “plate-rivet” pattern showed that in general the corrosion damage of joint No. 6R (in the connection with plates 6, 7 and 8) is approx. two times heavier than the damage of joint No. 3, and the riveted connection of plate 7 with the structural elements (skin, stringer), in comparison with the connection in plate 6, is practically completely worn out due to corrosion.

Subsequent connection disassembly and defect detection confirmed the efficiency of applying the offered AE testing method.

5.3.2 Control results of riveted connection condition at applied load

Besides controlling the bolt connections in the trials of helicopter structure resources, one of the tasks was also the evaluation of the defects of constructive node elements and compounds, including riveted connections. During testing of helicopter structure resources at the loading cycles 91 203...92 175, the change in the AE signal informative parameters, such as energy and cumulative energy (Fig. 5.22), indicated the presence of damage in the area of the left side frame No. 9 of the fuselage. In the research, second registration channel of the AE sensor was also informative. It was mounted on the helicopter fuselage and tail beam joint frame No. 1. The most considerable changes in energy and summar energy were fixed at 92 175 loading cycles.

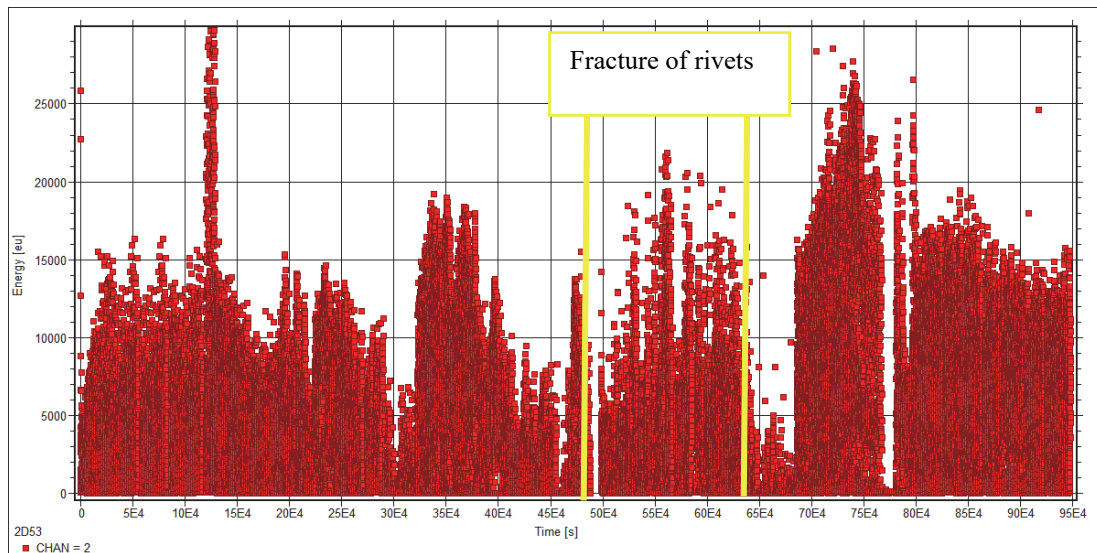


Fig. 5.22. Time-dependent changes in the AE signal energy (y axis), characterizing the defects of the rivets in joints.

During subsequent investigation, the raised AE signal source was identified – collapse of two rivets along the fuselage No. 9 on the left board in the area of stringers Nos 26 and 27 was found during regular inspection of the helicopter structure at the 91203 load cycle. They are marked accordingly, as crack No. 16 and No. 17. In the subsequent loading process at the load cycle 92175, six adjacent rivet collapses were recorded. The defects were labeled as cracks Nos 19–23. Fig. 5.23 depicts all the collapsed rivet fractures.

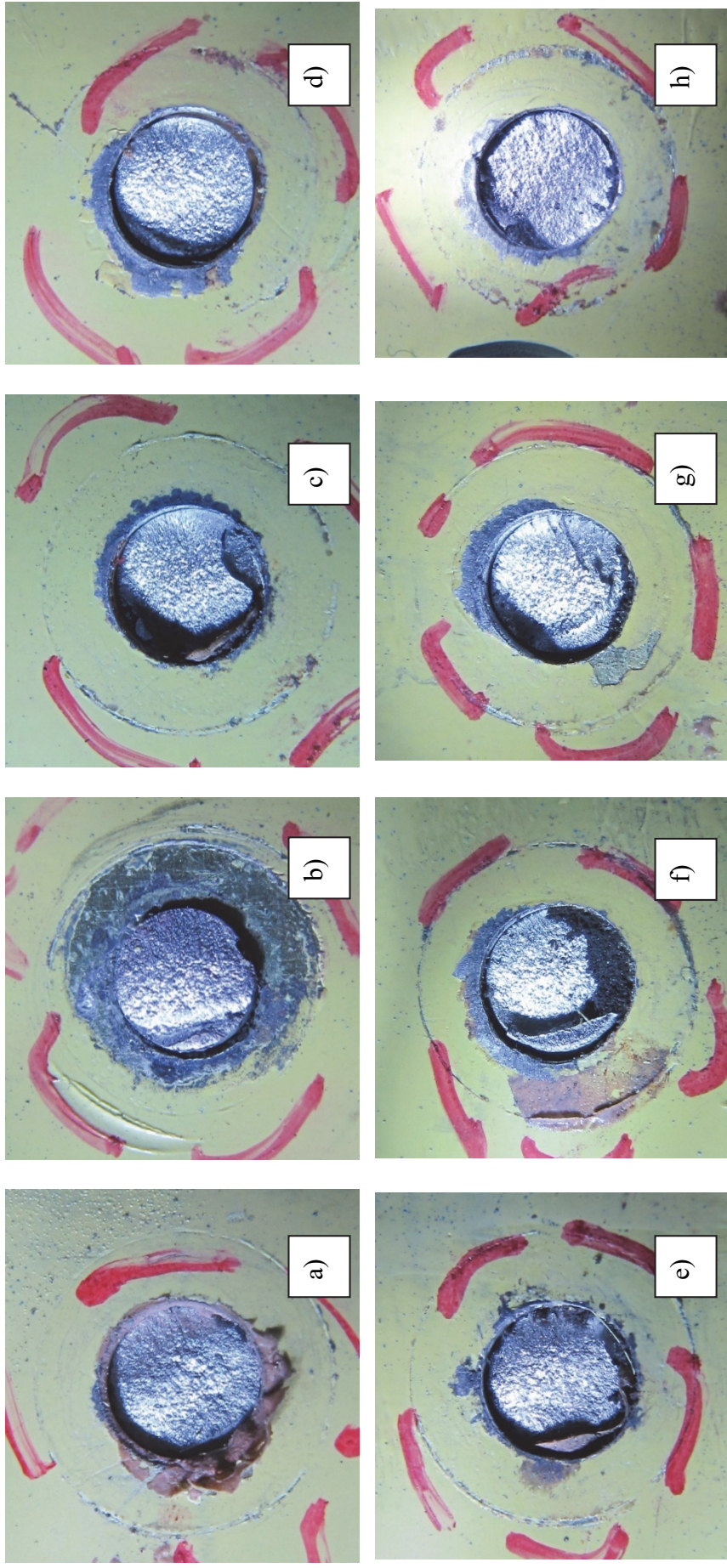


Fig. 5.23. Overview of the rivet material cracks after their collapse:

a) rivet No. 1 (crack No. 18); b) rivet No. 2 (crack No. 16); c) rivet No. 3 (crack No. 19); d) rivet No. 4 (crack No. 17); e) rivet No. 5 (crack No. 20); f) rivet No. 6 (crack No. 21); g) rivet No. 7 (crack No. 22); h) rivet No. 8 (crack No. 23).

CONCLUSIONS

1. Helicopter operational defect analysis allowed concluding that fatigue damage is the most dangerous in structural joints of aircraft structures. Non-destructive testing and diagnostics methods used during helicopter inspection do not provide information on the fatigue cracks and their development. There is a need to develop diagnostic methods for use on helicopters in operation in order to increase the safety of their structure.
2. Multi-channel acoustic emission measurement and data processing methodology were developed for structures defectology analysis at static and dynamic load conditions. AE sensor location was selected, taking into account the structural factors and the number of sensors. Hardware settings for AE measurements were developed through testing AE signal propagation parameter estimation. Methodology for AE signal processing, data visualization and AE source location was chosen taking into account structural elements of the helicopter, plating color effect, the overall noise level, parametric data, etc.
3. Mathematical model of fatigue defect localization in materials and structures was developed based on the AE measurement data. The model is based on the AE signal amplitude registration and analysis. It takes into account structural elements of the helicopter, and it can be applied using two or more AE sensors. Using this mathematical model it is possible to determine coordinates of the cluster where defect is located, center.
4. AE parameter informativity was assessed for metallic and composite structures under static and dynamic load conditions. Total AE was selected as a criterion for the assessment of damage accumulation of composite materials. The AE signal criteria – signal amplitude and the total AE – were selected in aluminum alloy sample tests. The character of AE amplitude was evaluated at the burst moment. The signal spectrum for the first AE signal originated in the crack development moment is analyzed. It is proven that the AE method is effective for the control of fatigue defects at an early stage and makes it possible to control the crack development process up to the fracture and assess the material load-bearing capacity.
5. Fatigue defect localization in the helicopter structure was experimentally determined by AE parameter – AE signal amplitude. Defect location is determined taking into account the real impact of structural elements. The amplitude attenuation coefficient used for defect localization in the helicopter structure that does not have structural elements is $K_{konstr} = 1$, but for the helicopter structure with structural elements such as stringers and frames K_{konstr} is in the range of 0.37–0.58.

6. The helicopter fuselage and tail boom joint bolt fatigue damage diagnostics with defect localization was performed during bench tests when, based on AE data, bolt fracture was expected. Bolt fracture was predicted at least 26 to 44 flight hours before the actual fracture. Using AE parameters, the microcracks origin intervals were identified when the bolt bearing capacity after the occurrence of the defect composed up to 96%. Such AE parameters as AE signal amplitude and absolute energy were correlated with the fracture kinetics. Analysis of AE parameters showed that the joint bolt tensioning torque directly impacts the fatigue defect spreading. The change in decreased tension momentum in relation to the required one slows down the crack development due to stress distribution. Fatigue surface analysis during fractographic research confirmed the AE measurement results.
7. Structural rivet and screw joining methodology was developed based on the AE measurements. The proposed method makes it possible to perform both the individual elements and the whole screw or rivet joint quality quantitative assessment in real structures in operation conditions.
8. Fractographic analysis of structural element fatigue surfaces was carried out, and AE parameter correlations with the fracture kinetics were identified. Defect sources were detected, and multi source structure was evaluated based on the fractographic analysis. Small-grained and coarse-grained areas characterizing the crack growth kinetics were observed in bolt fatigue fractures. Crack growth rate of bolt fractures at early stages was 80...90 nm/cycle, but afterwards reached on average 140...180 nm/cycle. Cracks in accelerated growth areas are characterized by slip zones. Performed spectral analysis indicated the presence of defects before bolt operation on the helicopter.

REFERENCES

1. Harbuz Y. *Aviācijas materiālu un konstrukciju noguruma bojājuma novērtējums uz akustiskās emisijas signālu mērījumu pamata*. Promocijas darba kopsavilkums. Rīga: RTU Izdevniecība, 2015, 33 lpp. ISBN 978-9934-10-740-5.
2. Hauka M. *Gaisa kuģu konstrukcijas inspekcijas plānošana*. Promocijas darba kopsavilkums. Rīga: RTU Izdevniecība, 2015, 29 lpp. ISBN 978-9934-10-664-4.
3. Kuzņecovs S. *Aviācijas alumīnija sakausējumu konstrukciju elementu tehniskā stāvokļa integrētā kontrole ar pjezoelektriskiem sensoriem*. Promocijas darba kopsavilkums. Rīga: RTU, 2011, 52 lpp.
4. Nasibullins A. *Akustiskās emisijas metodes pielietojuma izpēte aviotehnikas spēka konstrukciju kontrolei stendu izmēģinājumos*. Promocijas darba kopsavilkums. Rīga: RTU, 2011, 27 lpp. ISBN 978-9984-49-340-4.
5. Turko V. *Aviācijas konstrukciju noguruma agrīnās noteikšanas un kontroles metodes izstrāde stendu izmēģinājumos*. Promocijas darba kopsavilkums. Rīga: RTU Izdevniecība, 2013, 42 lpp. ISBN 9984-690-24-5.
6. Urbahs A., Carjova K., Urbaha M., Stelpa I., *Gaisa kuģu konstrukciju nesagraujošā kontrole*, iesniegts RTU Izdevniecībā 2016.
7. Urbahs A., Harbuzs J. *Aviācijas materiālu un konstrukciju noguruma bojājumu akustiskā kontrole*. Rīga: RTU Izdevniecība, 2015.
8. RĪGAS TEHNISKĀ UNIVERSITĀTE. *Konstrukciju skrūvju un kniežu savienojumu kombinētā akustiskās emisijas un ultraskaņas kontroles metode*. Aleksandrs Urbahs, Muharbijs Banovs, Margarita Urbaha, Kristīne Carjova, Jurijs Feščuks (izgudrotāji). Int. Cl.: G01N29/14. Iesniegšanas datējums: 2013-10-31. Patenti un Preču Zīmes. LV14971B. 2015-08-20.
9. Baldev Raj, Jayakumar T., Thavasimuthu M. *Practical Non-Destructive Testing*. Oxford: Alpha Science International Ltd, 2002, 200 pp. ISBN 9781842650813.
10. Bramwell A.R.S., Done G., Balmford D. *Bramwell's Helicopter dynamics*. 2nd edition. Great Britain: Bath Press, 2011, 373 pp. ISBN 0 7506 5075 3.

11. Hellier C.J. *Handbook of Nondestructive Evaluation*. USA: The McGraw-Hill Companies Inc, 2003, 594 pp. DOI: 10.1036/007139947X.
12. Johnson W. *Helicopter Theory*. New York: Dover publications Inc., 1994, 1089 pp. ISBN: 9780486682303.
13. Staszewski W.J., Boller C., Tomlinson G.R. *Health Monitoring of Aerospace Structures: Smart Sensor Technologies and Signal Processing*. Chichester: John Wiley & Sons, Ltd, 2004, 288 pp. ISBN: 0-470-84340-3.
14. United States. Federal Aviation Administration. *Nondestructive Testing in Aircraft*. Casper, WY: IAP Inc., 1989, 38 pp. ISBN: 0891000836.
15. Wanhill R.J.H. *Fatigue and fracture of aerospace aluminium alloys: a short course*. NLR TP 94034 L. Amsterdam, NLR Technical Publication, 1994.
16. Baxter M.G., Pullin R., Holford K.M., Evans S.L. Delta T source location for acoustic emission. **In:** *Mechanical Systems and Signal Processing*, Vol. 21, Iss. 3, 2007, pp. 1512–1520. <http://dx.doi.org/10.1016/j.ymsp.2006.05.003>
17. Birkelbah G., Grill W., Kuzņecovs S., Pavelko V. Integral Structural Health and Load Monitoring of a Helicopter Tail Boom Manufactured from Aluminum Sheet Metal with Support from Frames and Stringers by Guided Ultrasonic Waves. **In:** *SPIE Proceedings*, Vol. 8348, 2012, pp. 1–10. ISSN 0277-786X; Doi:10.1117/12.914970.
18. Boukabache H., Escriba C., Zedek S., Medale D., Rolet S., Fourniols J.Y. System-on-Chip Integration of a New Electromechanical Impedance Calculation Method for Aircraft Structure Health Monitoring. **In:** *Sensors*, Vol. 12, 2012, pp. 13617–13635. Doi:10.3390/s121013617.
19. Ciampa F., Feo M. A new algorithm for acoustic emission localization and flexural group velocity determination in anisotropic structures. **In:** *Applied Science and Manufacturing*, Vol. 41, Iss. 12, 2012, pp. 1777–1786.
20. Ciampa F., Feo M. A new wavelet based algorithm for impact identification and group velocity determination in composite structures. **In:** *Proceedings of the 5th European Workshop – Structural Health Monitoring 2010*, June 28 – July 4, Naples, Italy, 2010, pp. 1057–1063.

21. D. Vandenberg ground support equipment for the space shuttle. **In:** *AIAA meeting papers*, No. 294, 1981, pp. 1–28. DOI: 10.2514/6.1981-294.
22. Dragan K. Structural health monitoring and damage detection of the helicopter main rotor blades with the structure integrated sensors. **In:** *AIAC14 Fourteenth Australian International Aerospace Congress, 7th DSTO International Conference on Health & Usage Monitoring (HUMS-2011)*, 2011, pp. 1–8.
23. Finlayson R.D., Friesel M., Carlos M., Cole P., Lenain J.C. Health monitoring of aerospace structures with acoustic emission and acousto-ultrasonics. **In:** *Insight*, Vol. 43, No. 3, 2001, 4 pp.
24. Hill R., Stephens R.W.B. Sonic emission during deformation of solids. **In:** *Arch. Akust.*, Vol. 6, No. 1, 1971, pp. 187–221.
25. Hutton P. H., Skorpik I. R. In-flight fatigue crack monitoring using acoustic emission. **In:** *ISA Trans*, Vol. 20, No. 1, 1981, pp. 79–83.
26. Mizutani Y., Saiga K., Nakamura H., Takizawa N., Arakawa T., Todoroki A. Integrity evaluation of COPVs by means of acoustic emission testing. **In:** *Acoustic Emission*, Vol. 26, 2008, pp. 109–119.
27. Nasibullins A., Urbahs A., Banov M. Acoustic Emission Monitoring of Fatigue Crack Origination during Titanium Specimens Tests. **In:** *Intelligent Transport Systems*, Vol. 34, 2010, pp. 61–67. ISSN 1407-8015.
28. Paramonovs J., Chatys R., Andersons J., Kleinhofs M. Markov Model of Fatigue of a Composite Material with Poisson Process of Defect Initiation. **In:** *Mechanics of Composite Materials*, Vol. 48, Iss. 2, 2012, pp. 217–228. ISSN: 0191-5665.
29. Parrish B. Acoustic emission techniques for in-flight structural monitoring. **In:** *SAE technical paper series N801211*, 1980, p. 8. DOI: 10.4271/801211.
30. Pavelko V. Application of the Fatigue Crack Opening/Closing Effect for SHM Using Electromechanical Impedance Technology. **In:** *Applied Mechanics and Materials*, Vol. 811, 2015, pp. 228–235. ISSN 1660-9336; e-ISSN 1662-7482.
31. Pavelko V. Electromechanical Impedance for SHM of Aircraft Bolted Joints. **In:** *SPIE Proceedings*, Vol. 8694, 2013, pp. 1–14. ISSN 0277-786X; Doi:10.1117/12.2009588.

32. Pavelko V., Pfeifer H., Wevers M. Fatigue Crack Open Effect to Lamb Waves in Thin Al Sheet. **In:** *International Review of Aerospace Engineering (I.RE.AS.E)*, Vol. 4, No. 3, 2011, pp. 173–179. ISSN: 1973-7459.
33. Pollock A.A. Acoustic Emission Inspection. **In:** *Metals Handbook*, Vol. 17, 9th edition, 1989, pp. 278–294.
34. Schütz W.H. A History of Fatigue. **In:** *Engineering Fracture Mechanics*, Vol. 52, No. 2, 1996, pp. 263–270,
35. Shaniavski A., Urbahs A., Banovs M., Nasibullins A., Carjova K. Analysis of the Mechanism of Destruction of Aircraft Components. **In:** *International Congress on Engineering and Technology: Proceedings, 25–27 June 2013, Dubrovnik*, pp. 167–172. ISBN 9788087670088.
36. Šanjavskis A., Urbahs A., Banovs M., Doroško S., Hodoss N. Correlation of Acoustic Emission Signals with Kinetics of Fatigue Crack Growth in the Shock Absorber of Aircraft Landing Gear. **In:** *Transport. Aviation Transport*, Vol. 31, 2009, pp. 94–100. ISSN 1407-8015.
37. Tatro C.A., Liptai R.G., Harris D.O. Acoustic emission technique in material research. **In:** *Nondestructive Testing*, Vol. 3, No. 3, 1971, pp. 215–275.
38. Urbach A., Banov M., Turko V. Hypothesis of local zones with dependent fatigue damages accumulation. **In:** *3rd International Conference on Mechanical and Aerospace Engineering, ICMAE 2012*, July 7–8, Paris, France, 2012, pp. 19–23.
39. Urbahs A., Andrejevs S. The Problem of Vibro-Acoustic Diagnostics of Gas Turbine Engine Bearing Units. **In:** *Mechanika 2015: Proceedings of the 20th International Conference*, Lithuania, Kaunas, 23–24 April, 2015. Kaunas: Kaunas University of Technology, 2015, pp. 268–271. ISSN 1822-2951.
40. Urbahs A., Banov M., Carjova K., Fescuks J. Structural health monitoring of helicopter bolted and riveted joints by acoustic emission method. **Submitted in:** *Aerospace Science and Technology*, 2016.

41. Urbahs A., Banov M., Doroško S., Harbuz Y., Turko V. Acoustic Emission Diagnostics of Fatigue Crack Development during Undercarriage Bench Testing. **In:** *Mechanika 2010: Proceedings of 15th International Conference*, Lithuania, Kaunas, 8–9 April, 2010. Kaunas: Kaunas University of Technology, 2010, pp. 450–454.
42. Urbahs A., Banov M., Harbuz Y., Feščuks J., Sologubovs J. Evaluations of Degree of Damage and Probability of Forecasting of Destructing Load in Anisotropic Composites by Means of Acoustic Emission in Materials under Static Loading. **In:** *Transport Means 2011: Proceedings of the 15th International Conference*, Lithuania, Kaunas, 20–21 October, 2011. Kaunas: Kaunas University of Technology, 2011, pp. 270–273. ISSN 1822-296X.
43. Urbahs A., Banov M., Harbuz Y., Turko V., Feshchuk Y., Khodos N. Investigation of Mechanical Properties of Composite Materials Using the Method of Acoustic Emission. **In:** *Mechanika 2011: Proceedings of the 16th International Conference*, Lithuania, Kaunas, 7–8 April, 2011. Kaunas: Technologija, 2011, pp. 306–310. ISSN 1822-2951.
44. Urbahs A., Banov M., Turko V. The Fatigue Damage Accumulation on Systems of Concentrators. **In:** *World Academy of Science, Engineering and Technology*, Vol. 5, No. 11, 2011, pp. 934–939. ISSN 2010-376X. e-ISSN 2010-3778.
45. Urbahs A., Banov M., Turko V. The Fatigue Damage Accumulation on Systems of Concentrators. **In:** *World Academy of Science, Engineering and Technology*, Vol. 5, No. 11, 2011, pp. 934–939. ISSN 2010-376X. e-ISSN 2010-3778.
46. Urbahs A., Banov M., Turko V., Feshchuk Y., Khodos N. Investigation of Micromechanics of Plasto-Elastic Behaviour of Anisotropic Composite Materials under Static Loading by the Acoustic Emission Method. **In:** *Advances and Trends in Engineering Materials and Their Applications: Conference Proceedings*, Latvia, Riga, 11–15 July, 2011. Canada: University of Ottawa, 2011, pp. 1–10. ISBN 978-0-9866504.
47. Urbahs A., Banov M., Turko V., Savkovs K., Feshchuk Y., Carjova K. Research into the Micromechanics of the Plactic-Elastic Behaviours of Anisotropic Composite Materials under Static Loading by the Acoustic Emission Method. **In:** *17th International Conference “Mechanics of Composite Materials – 2012”*: Book of Abstracts, Latvia, Jūrmala, 28 May – 1 June, 2012. Riga, 2012, pp. 221–221.

48. Urbahs A., Banov M., Turko V., Sologubovs J. Investigation of the Fatigue Cracks Origin Dependence on the Specimens with Numerous Concentrators. **In:** *Proceedings of 13th International Conference "Maritime Transport and Infrastructure"*, Latvia, Riga, 28–29 April, 2011. Riga: Latvian Maritime Academy, 2011, pp. 170–173.
49. Urbahs A., Banovs M., Carjova K., Turko V. The Characteristic Features of Composite Materials Specimen's Static Fracture Investigated by the Acoustic Emission Method. **In:** *Applied Mechanics and Materials*, Vol. 232, 2012, pp. 28–32. ISSN 1660-9336; DOI:10.4028/www.scientific.net/AMM.232.28.
50. Urbahs A., Banovs M., Carjova K., Turko V., Feshchuk J. Research of the micromechanics of composite materials with polymer matrix failure under static loading by the acoustic emission method. **Submitted in:** *Aviation*, 2016.
51. Urbahs A., Banovs M., Harbuz Y., Turko V., Khodos N., Feščuks J. Estimation of Mechanical Properties of the Anisotropic Reinforced Plastics with Application of the Method of Acoustic Emission. **In:** *Transport and Telecommunication*, Vol. 11, No. 2, 2010, pp. 68–75. ISSN 1407-6160; e-ISSN 1407-6179.
52. Urbahs A., Banovs M., Turko V., Feshchuk Y. Diagnostics of Fatigue Damage of Gas Turbine Engine Blades. **In:** *WASET*, Issue 59 (part IX), 28–30 November, 2011. Venice: WASET, 2011, pp. 906–911.
53. Urbahs A., Banovs M., Turko V., Feshchuk Y. Diagnostics of Fatigue Damage of Gas Turbine Engine Blades. **In:** *WASET*, Issue 59 (part IX), 28–30 November, 2011. Venice: WASET, 2011, pp. 906–911.
54. Urbahs A., Banovs M., Turko V., Feshchuk Y. New Approach to Use the Acoustic Emission Monitoring for the Defects Detection of Composit-Material's Design Elements. **In:** *Ūdens Transports un infrastruktūra: 14. starptautiskā konference*, Latvia, Riga, 26.–27. aprīlis, 2012,– pp. 45–50.
55. Urbahs A., Carjova K. Research on bolting elements of helicopter fuselage and tail boom joints using acoustic emission amplitude and absolute energy criterion. **Submitted in:** *Advances in Acoustics and Vibration*.
56. Urbahs A., Carjova K., Feščuks J., Lama M. Research on Aluminium alloys static testing using Acoustic Emission testing. **Submitted in:** *Mechanika 2016*.

57. Urbahs A., Carjova K., Feščuks J., Stelpa I. Analysing the results of acoustic emission diagnostics of a structure during helicopter fatigue tests. **Submitted in:** *Aviation 2016*.
58. Urbahs A., Carjova K., Feščuks J., Stelpa I. Development of Theoretical Model for Aircraft Structural Health Monitoring by Acoustic Emission Method. **In:** *Mechanika 2015: Proceedings of the 20th International Conference*, Lithuania, Kaunas, 23–24 April, 2015. Kaunas: Kaunas University of Technology, 2015, pp. 262–267. ISSN 1822-2951.
59. Urbahs A., Carjova K., Nasibullins A., Feščuks J. Research on fatigue fracture kinetics of helicopter fuselage bolting elements. **Submitted in:** *Transport Means 2016: Proceedings of the 20th International Conference*.
60. Urbahs A., Carjova K., Nasibullins A., Nedelko D., Millere E. Research on AE signal propagation in helicopter structural elements. **Submitted in:** *Transport and Aerospace engineering 2016*.
61. Urbahs A., Carjova K., Urbaha M. Acoustic emission criterion during dynamic test of Aluminium alloys. **Submitted in:** *2016 AES-ATEMA International Conference “Advances and Trends in Engineering Materials and their Applications”*.
62. Urbahs A., Carjova K., Urbaha M. Acoustic emission diagnostics of fuselage and tail boom jointing bolts during helicopter bench tests. **Submitted in:** *ICAETM 2016: 18th International Conference on Aviation Engineering, Technology and Management*.
63. Urbahs A., Harbuz Y., Urbaha J. Evaluating of Damageability of Materials at Fatigue Loading Based on Signals of Acoustic Emission. **In:** *Mechanika 2015: Proceedings of the 20th International Conference*, Lithuania, Kaunas, 23–24 April, 2015. Kaunas: Kaunas University of Technology, 2015, pp. 257–261. ISSN 1822-2951.
64. Urbahs A., Shaniavsky A., Doroško S., Banov M. Correlation of Acoustic Emission and Fractographic Characteristics during Fatigue Crack Development. **In:** *Proceedings of the 29th European Conference on Acoustic Emission Testing*, 8–10 September, 2010. Vienna: European Working Group on Acoustic Emission, 2010, pp. 20–27.
65. Urbahs A., Shanyavskiy A., Banovs M., Carjova K. Evaluation of an Acoustic Emission Criterion of Under Surface Fatigue Cracks Development Mechanism in Metals. **In:** *Transport Means 2012: Proceedings of the 16th International Conference*, Lithuania, Kaunas, 25–26 October, 2012. Kaunas: Technologija, 2012, pp. 131–134. ISSN 1822-296X.

66. Urbahs A., Valberga A., Banovs M., Carjova K., Stelpa I. The Analysis of Efficiency of Acoustic Emission Diagnostic Method for the Determination of Defect Coordinates **In:** *Transport and Aerospace Engineering*, Vol. 1, 2014, pp. 32–36. ISSN 2255-968X; Doi:10.7250/tae.2014.006.
67. Vainberg V.E. Determination of the coordinates of an acoustic emission source in two and three dimensional spaces without the aid a computer **In:** *The Soviet Jjournal of Non-Destructive Testing*, Vol. 17, Iss. 6, 1981, pp. 473–477.
68. Ziegler F. Acoustic emission from Plastic source **In:** *Journal of Computational Acoustics*, 2001, vol. 9, issue 4, pp. 1329-1345 DOI: 10.1142/S0218396X01001182
69. Friesel M.A., Barga R.S., Dawson J.F., Hutton P.H., Kurtz R.J., Lemon D.K. Acoustic emissions applications on the NASA space station. [Online.] *Digital Commons*, [19 July 2013]. Available at: <http://lib.dr.iastate.edu/cgi/viewcontent.cgi?article=2982&context=qnde>
70. Muravin B. Acoustic wave propagation and source location. [Online.] Available at: <http://www.muravin.com/> [Accessed on Jan. 15, 2014.]
71. Pocket AE-2™: Portable 2-Channel Acoustic Emission System: Mistras. A world of NDT solutions. [Online.] Physical Acoustics Cooperation, 2010. Available at: http://www.pacndt.com/downloads/Pocket%20AE-2_46-06.pdf [Accessed on 17 May 2014.]
72. Prosser W., Gorman M., Madaras E. Acoustic emission detection of impact damage on space shuttle structures. [Online.] NASA Technical reports server. Available at: <http://ntrs.nasa.gov/archive/nasa/casi.ntrs.nasa.gov/20040171467.pdf> [Accessed on 20 July 2013.]
73. The Difference Engine: Old before their time. [Online.] *The Economist Newspaper Limited*, 2011 Available at: http://www.economist.com/blogs/babbage/2011/04/aircraft_fatigue [Accessed on 20 July 2013.]
74. RIGAS TEHNISKA UNIVERSITATE. *A method for renovation of steel precision pair parts.* Urbahs A., Savkovs K., Urbaha M., Nesterovskis V., Carjova K., Urbaha J., Kuļšovs N. Int. Cl.: C23C14/02, B23P6/00, C23C14/06, C23C14/34, C23C14/58. Application date: 2013-09-19. Patenti un Preču Zīmes. EP2851450. 2015-03-25.
75. Eisenblatter I. Schall emissions analyse. Ein neues zerstörungsfreies Prüfverfahren. **In:** *Ing. Dig*, Bd. 11, N. 10, 1972, s. 62–67.

76. *Вертолет Ми 8. Анализ конструктивно производственных и эксплуатационных дефектов Вертолета Ми 8.* Ленинград, 1977.
77. *Вертолет Ми-2. Техническое описание. Книга 1: Конструкция вертолета.* ВСК Свидник, 1970, 128 с.
78. *Вертолет Ми-24В (Ми-24Д). Инструкция по технической эксплуатации,* 1982.
79. *Вертолет Ми-26Т. Руководство по технической эксплуатации. Книга 2: Планер, Часть 1,* Москва: Транспорт, 1987, 462 с.
80. *Вертолет Ми-26Т. Руководство по технической эксплуатации. Книга 2: Планер, Часть 2,* Москва: Транспорт, 1987, 495 с.
81. *Вертолет Ми-8. Техническое описание, Книга 2: Конструкция,* 2000.
82. Грешников В.А., Дробот Ю.Б. *Акустическая эмиссия.* Москва: Изд-во стандартов, 1976, 272 с.
83. Дробот Ю.Б., Лазарев А.М. *Неразрушающий контроль усталостных трещин акустико-эмиссионным методом.* Москва: Изд-во стандартов, 1987, 128 с.
84. Епифанцев Ф.И. *Вертолет Ми-6. Инструкция по эксплуатации и техническому обслуживанию. Планер и силовая установка.* 1970.
85. Карзов Г.П., Марголин Б.З., Швецова В.А. *Физико механическое моделирования процессов разрушения.* Санкт Петербург: Политехника, 1993, 391 с.
86. Кубарев А.И. *Надежность в машиностроении.* Москва: Издательство стандартов, 1977, 264 с.
87. Миль М.Л., Некрасов А.В., Браверман А.С., Гродко Л.Н., Лейканд М.А. *Вертолеты. Расчет и проектирование. Том 2. Колебания и динамическая прочность.* Москва: Машиностроение, 1967. 424 с.
88. Миль М.Л., Некрасов А.В., Браверман А.С., Гродко Л.Н., Лейканд М.А. *Вертолеты. Расчет и проектирование. Том 1. Аэродинамика.* Москва: Машиностроение, 1967, 455 с.
89. Миртов К.Д., Черненко Ж.С. *Конструкция и прочность самолетов и вертолетов.* Учебник для вузов гражданской авиации. Москва: Транспорт, 1972, 439 с.

90. Михеев Р.А. *Прочность вертолетов*. Москва: Машиностроение, 1984, 280 с.
91. *Программа сертификационных испытаний на усталость хвостовой балки кия вертолета*. Aviatest LNK, 2014.
92. Трипалин А.С., Буйло С.И. *Акустическая эмиссия. Физико механические аспекты*. Ростов на Дону: изд-во Ростовского ун-та, 1986, 160 с.
93. Урбах А.И. *Диагностика повреждений и прогнозирование разрушений авиационных конструкций акустико-эмиссионным методом*. Рига: РАУ, 1996, 122 с.
94. Шанявский А.А. *Безопасное усталостное разрушение элементов авиаконструкций синергетика в инженерных приложениях*. Уфа: Монография, 2003, 802 с.
95. Шанявский А.А. *Безопасное усталостное разрушение элементов авиаконструкций*. Уфа: Изд-во науч.-техн. лит. „Монография”, 2003, 802 с.
96. Бородин Ю.П. Техническая диагностика конструкции планера самолета с использованием метода акустической эмиссии. **В кн.:** РГУ, ч. 2, 1984, с. 91–92.
97. Акустико-эмиссионные системы Лель/А-LINE 32D (DDM). [Online.] Группа компаний „ИНТЕРЮНИС”, 2013. Available at: <http://www.interunis.ru/ru/produkcziya-a-line-32d/ae-sistemyi/ddm.html> [Accessed on 27 May 2014.]
98. Rīgas Tehniskā universitāte. *Akustiskās emisijas avotu koordinātu noteikšanas paņēmiens*. Aleksandrs Urbahs, Kristīne Carjova, Jurijs Feščuks, Margarita Urbaha (izgudrotāji). Int. Cl.: Iesniegšanas datējums: 2016-04-26. Patenti un Preču Zīmes.